Technische Universiteit Delft

Ship Motion Predictions in the Time Domain

using identified linear and non-linear force coefficients

S.G. de Haan

TU Delft

Ship Motion Predictions in the Time Domain

using identified linear and nonlinear force coefficients

by

S.G. de Haan

to obtain the degree of Master of Science
at the Delft University of Technology,

Report number: MT.21/22.023.M
Student number: 4240227

Thesis committee:

Prof. dr. ir. I. Akkerman,	TU Delft
Dr. P. Naaijen,	TU Delft, supervisor
Dr. M. Kok,	TU Delft
Ir. R. Paravastu,	Next Ocean Corporation

TU Delft

Abstract

Deterministic predictions of wave induced ship motion are increasingly often used to enlarge the operational envelope of ships that perform complex operations at open sea. The large amount of complex operations performed nowadays, motivates the relevance of motion predictions. The company Next Ocean provides these forecasts, based on linear seakeeping theory. While highly linear degrees of freedom are predicted accurately, roll motion predictions prove to be more demanding and are less accurate. This research aims to improve roll prediction accuracy by adding (non)linear damping to the equations of motion. The prediction optimization is performed on data of the platform supply vessel Acta Auriga.

To enable the use of nonlinear forces, the equations of motions are first implemented in the time domain using Cummins' equations. The linear coefficients in this equation are determined from the frequency dependent coefficients in Acta Auriga's hydrodynamic database. To ensure the correctness and investigate the limitations of the implemented Cummins equation, the results from the time and frequency domain are extensively compared. Both monochromatic excitations, as well as spectrum (JONSWAP) excitations are considered. In contrast to linear force coefficients, nonlinear force coefficients are generally not known for a given vessel. Implementing these forces into the equations of motion imposes the need for an approximation of these coefficients. Estimates for the linear, quadratic and cubic viscous damping forces are made, using both the measured motions of a vessel operating at sea and the predictions of the corresponding excitation force, made by Next Ocean. A multivariate regression algorithm is used for the identification.

The Cummins equation was successfully implemented. However, the translation from frequency to time domain was more error prone than anticipated; the frequency dependent coefficients need to meet requirements that are typically not met by databases meant for frequency domain calculations only. Furthermore, degrees of freedom without a restoring force showed running away behaviour that could not be negated without adding extra damping. The roll motion was susceptible to instabilities. The exact origin of this instability was looked for, but could not be found. Adding damping resolved the instability. Furthermore, the interpolation in the roll response amplitude operator introduced errors in the initialisation of time domain calculations, which led to inaccurate results when spectrum excitations corresponding to more severe sea states were used. Only under specific conditions, these high energy spectra led to accurate roll predictions. Adding damping made for a close match between frequency and time domain calculation for all degrees of freedom. The complexities mentioned made that an easily scalable algorithm could not be obtained using time domain calculations. Easy scalability being important to Next Ocean means that running time domain simulations in Next Ocean's product is deemed unrealistic. This also means that no nonlinear forces can be used in real time applications.

In an attempt to improve linear predictions, coefficients in the linear seakeeping model, including the linear damping coefficient, are identified and vessel motions are re-predicted with the added damping and updated linear force coefficients, using the Cummins equation. None of the identified parameters led to better predictions than were obtained by Next Ocean. Identifying and updating parameters was therefore concluded to be not beneficial to the quality of the motion predictions. Adding a fixed amount of linear roll damping, which was not identified from the field data, did lead to improved prediction quality; correlations between predictions and measurements increased by 9.6%.

While the motion prediction could not be improved using the Cummins equation, valuable information on the time domain simulations was obtained. The finding that better predictions were consistently obtained by adding a fixed amount of damping, sparks an opportunity for further research into the ideal amount of damping. This, and more elaborate identification schemes could provide meaningful insight to improve motion predictions.

Preface

Before you lies my graduation report, *Ship Motion Prediction in the Time Domain, Using Identified Force Coefficients*, which was written to obtain the degree of Master of Science. This report is the last ordeal in reaching that goal. I performed the research that lies at the basis of this report at the startup company Next Ocean in Delft, under supervision of Peter Naaijen.

Over the duration of the project, I have learned many things; about vessel motions and their modelling, but also about myself. For that I would like to thank my colleagues to be at Next Ocean; Peter Naaijen, Karel Roozen, Raghu Paravastu and Yperion Bristogiannis, for the entertaining and stimulation times we had. Especially Peter; thanks for being understanding and compassionate in lesser times.

Yuki and Noor, many thanks for all the support. I could not have done this without you.

Remember; nonlinear is not straight forward!

S.G. de Haan
Den Haag, March 2022

Contents

1 Introduction **1**
1.1 Background . . . 1
1.2 Problem Statement . . . 2
1.3 Research Objectives . . . 2
1.4 Report Structure . . . 3

2 Theory and Implementation **5**
2.1 Introduction . . . 5
2.1.1 General Linear Seakeeping . . . 5
2.1.1.1 **The Equation of Motion** . . . 6
2.1.1.2 **Coupling Between Degrees of Freedom** . . . 6
2.1.1.3 **Frequency Dependent Coefficient Matrices** . . . 7
2.2 Frequency Domain Model . . . 8
2.2.0.1 **A Motion Transfer Function** . . . 8
2.3 Time Domain Model . . . 9
2.3.0.1 **Cummins Equation** . . . 9
2.3.0.2 **Cummins and the Hydrodynamic Database** . . . 11
2.3.0.3 **Solving the Convolution Integral** . . . 11
2.3.0.4 **Retardation Based on Added Mass** . . . 12
2.4 Coefficient Identification . . . 13
2.5 Cummins Implementation . . . 14
2.5.1 The Retardation Function . . . 14
2.5.2 Infinite Frequency Added Mass . . . 15
2.5.3 Implementing the Retardation Convolution . . . 15

3 Results **17**
3.1 Cummins Equation . . . 17
3.1.1 Uncoupled motion, Single Frequency Excitation . . . 17
3.1.1.1 **Zero Initial Position and Velocity** . . . 17
3.1.1.2 **Matching Initial Conditions** . . . 18
3.1.1.3 **A Closer Look at Surge, Sway and Yaw** . . . 19
3.1.1.4 **Roll Free Decay Instability** . . . 21
3.1.1.5 **Steady State Error** . . . 24
3.1.2 Uncoupled Motions, Spectrum Excitation . . . 24
3.1.2.1 **Interpolation in the Roll RAO** . . . 25
3.1.3 Coupled Motions, Single Frequency Excitation . . . 28
3.1.3.1 **Poor Tail Fitting** . . . 28
3.1.3.2 **Steady State Errors** . . . 30
3.1.4 Coupled Motions, Spectrum Excitation . . . 32
3.2 Parameter Identification and Re-Prediction . . . 32
3.2.1 Field Data Processing . . . 32
3.2.1.1 **Field Data Segments** . . . 33
3.2.1.2 **Scaling the Excitation** . . . 34
3.2.1.3 **Shifting the Excitation** . . . 34
3.2.2 Re-predicting, No Identification . . . 34
3.2.3 What Coefficients to Identify . . . 36
3.2.4 Re-predicting, With Identification . . . 38
3.2.4.1 **Performance with Identified Coefficients Other Than Damping** . . . 39

4 Discussion and Conclusion **41**
4.1 Time Domain Modelling 41
4.2 Identification and Re-Prediction 42
4.3 Overall Conclusions and Recommendations 43

A RAO Phase **45**

B Damping, Retardation and Added Mass **47**

C Force and Moment Residuals **53**

D Correlation Coefficients of Re-Predictions with Identified Coefficients **55**

List of Figures

2.1 The six degrees of freedom depicted 5
2.2 Roll damping in the hydrodynamic database, and an exponential tail fitted to the high frequency part of the curve. 15
2.3 Roll retardation function. 15
2.4 Roll infinite frequency added mass stabilises for higher frequencies, while showing very slight wiggles at lower frequencies. 16

3.1 The most simple Cummins implementation results; uncoupled degrees of freedom, single frequency excitation and zero initial conditions. DS in the legend stands for Domain Simulation. 18
3.2 More elaborate initial conditions made for a closer match between time and frequency domain results. A past velocity is provided to load the damping and both initial position and velocity match the frequency domain solutions. The transient period is as good as gone. 19
3.3 All degrees of freedom without a restoring force show running away behaviour. This graph shows how this motion can even accelerate with time. These predictions were made in the time domain. 19
3.4 Sway retardation functions with different amounts of frequency independent damping and varying fitted high frequency tails. 21
3.5 Free decay motions of heave, roll and pitch.Heave and pitch both show a nicely decaying curve. The roll motion however does not decay with time. 22
3.6 The phase between the force created by the retardation function and the velocity, for roll. The natural frequency lays between the two purple lines. 23
3.7 The total energy in the free decaying roll motion; it increases with time. 23
3.8 The difference between the time and frequency domain motion amplitudes. Positive values indicate that the time domain amplitudes were higher than the frequency domain amplitudes. The running away behaviour of surge, sway and yaw was corrected for to obtain sensible values for the amplitude error. 24
3.9 Uncoupled degrees of freedom, spectrum excitation response. 25
3.10 More severe sea states make the roll response to a spectrum excitation deviate from frequency domain results. 26
3.11 A cross section off the Roll RAO, note the extreme peak at the resonance frequency. . . 26
3.12 Different interpolation schemes, along with the reconstructed RAO, show how linear interpolations introduces errors in the motion amplitude of the past velocities provided to initialise the roll calculation. 27
3.13 The roll RAO in the complex plane. Note the extreme absolute value of the roll RAO; the red crosses are the only points at the extreme distance from the origin. Other DOF's show a much more curved, less extreme RAO. 28
3.14 The added damping closes the gap between time and frequency domain results. Note the changing motion amplitude by adding damping. 28
3.15 The dampingcurve for the crossterm between surge and heave. 29
3.16 From the damping shown in figure 3.15, these retardation function were obtained. Note that the oscillations persist for high τ values. 29
3.17 From the retardations shown in figure 3.16, these added mass curves were obtained; It is much less clear what value to choose for A_∞. 30
3.18 The steady state difference between frequency and time domain amplitudes of coupled motions. The error is determined as a percentage with respect to the frequency domain results, as was done for figure 3.8. 31

3.19 Coupled degrees of freedom exposed to a spectrum excitation are the most realistic type of synthetic experiments. 32
3.20 Scaling factor deviate only slightly through a section of time. Heave and pitch show similar scaling factors. 33
3.21 The shifting of the predicted signals ensures an as good as possible prediction. 34
3.22 The time domain re-prediction, without updated or added coefficients. 35
3.23 The correlations of the time domain re-predictions are considerably lower then those obtained by Next Ocean, especially for roll. 36
3.24 Roll moment residuals. Each dot represents a measurement. The title of each sub-graph is the correlation coefficient. 37
3.25 The identified roll damping coefficients show a wide variation. 38
3.26 Correlation coefficients of the re-predicted roll motions, using identified linear roll damping. 38
3.27 Adding a fixed amount of linear damping led to improved results, compared to predictions performed by Next Ocean. 39
3.28 Adding the fixed amount of damping also visually improves the prediction quality. 39

A.1 Phase differences between time and frequency domain calculations. Values are in percentages. This is the percentage of the difference, relative to the frequency domain value. This also holds for the figure containing the differences of the uncoupled motions 46

D.1 Identification of a sway acceleration induced roll moment. 55
D.2 Identification or a roll acceleration induced roll moment. 56
D.3 Identification of a roll position induced roll moment. 56
D.4 Identification of a pitch velocity induced pitch moment. 56
D.5 Identification of added roll damping, linear, quadratic and cubic. Note the gaps in the re-predicted motion correlations. Negative damping has been identified and added in those segments, leading to unstable simulations. 57

1 Introduction

1.1. Background

During many operations at sea, ship motions are of decisive importance. Keeping vessel motions under a certain threshold ensures safety and prevents loss or damage of materials. During the design phase of a ship, attention can be paid to sea keeping by use of models that predict the response in a given sea state. However, also during the ships lifespan, predictions of the vessel motions are of importance. An increasing amount of complex operations at sea drives the search for more accurate predictions of wave induced motions. A complex operation can mean a multitude of undertakings and examples include hoisting a load from or on board a platform supply vessel, landing a helicopter on a ship at open sea and placing an offshore windmill [5]. Many more operations could be placed in this list, they have in common that they can be endangered by too severe motions. Motion predictions can also be of use for more modern floating structures. Large floating windmills as well as Wave Energy Converters can experience excessive structural loads when large waves hit. Foreseeing these loads is of value since these structures can alter their moving parts, making them more efficient in converting energy and better suited to resist excessive motions [4],[14].

During and shortly before operations, multiple techniques can be used to create predictions or expectations for the upcoming vessel motions. These techniques have different working principles. An often used method is based on statistics. The wave spectrum can be measured with a nearby wave buoy, determined from vessel motions [10], [16], [18], or measured from radar images, [7],[19],[2]. From this wave spectrum, a motion spectrum can be obtained. From there, probabilities of exceedance of chosen thresholds can be determined. The decision on whether or not to undertake the operation is based on these probabilities. A requirement might for example be that in the 3 minutes to come, the chance that the vertical displacement exceeds 2 meters cannot be larger than one in a thousand. A property of this often used technique based on statistics is that, given a certain sea state and safety requirement, a certain operation can either be executed or not. This means that as long as the sea state does not change, a certain operation can, or can not, be executed. During periods where the sea state is too severe to execute an operation, many periods long enough to perform the operation safely will occur. In fact, at the threshold sea state in the above example, during the vast majority of the three minute periods, the motion threshold is not exceeded. This illustrates that uptime may be lost by using this statistical method. A relatively new, and more elaborate method is to use deterministic motion predictions.

Deterministic motions predictions are not based on wave or motions spectra, and are therefore not based on statistics. Instead, a ‘measurement’ of the surrounding wavefield is made. This wavefield is then analyzed and expressed as a sum of wave components. This makes it possible to calculate how the wavefield at a given moment will evolve in time. From this, the loads exerted by the waves on the ship can be determined, ship motions are determined from these loads. Using this method, motions a few minutes into the future can be predicted. This is a fundamentally different way to predict wave induced motions than the statistically based method described above. The advantage of this technique

is the possibility to distinguish between more and less intense moments, while being exposed to a wave spectrum that would otherwise have canceled the operation altogether. Using deterministic prediction could therefore enlarge the operational envelope.

1.2. Problem Statement

This master graduation project was done at the startup company Next Ocean. Next Ocean makes deterministic wave predictions, using the noise in navigational radar images [8], [15]. These images contain information of the steepness of the waves, from which the wavefield surrounding the vessel can be constructed, without the need of wave buoys. Next Ocean uses linear seakeeping theory in the frequency domain to obtain the ship motions from the wave field. For most degrees of freedom this works well.

Roll predictions tend to perform considerably. The roll motion response to excitation differs from other degrees of freedom. This stems from the fact that roll has relatively little damping. The theory behind Next Ocean's motion predictions accounts for potential damping only, thereby neglecting friction damping. This while friction damping plays a relatively large role for roll. Adding linear damping to counteract this underprediction of damping force is often done. However, friction damping is considered to be, at least partly, a quadratic function of fluid velocity. This nonlinear force cannot be incorporated in the frequency domain model used by Next Ocean.

The importance of motion predictions has been elaborated on, and much progress has been made the past years. The lacking performance of the roll prediction is however an issue that deserves revisiting; this project is aimed at increasing roll prediction performance.

1.3. Research Objectives

The main research objective is to investigate if roll predictions can benefit from added nonlinear damping. A side goal is to gain insight into whether motion predictions for other degrees of freedom can improve from updating already present force coefficients. Multiple sub objectives have been defined that will lead to conclusions regarding the main objective. The sub objectives are listed below.

1. Implement the Cummins equation. The Cummins equation is the time domain equivalent of the earlier mentioned equations of motion in the frequency domain. A translation from the frequency dependent force coefficients to coefficients in the time domain model needs to be made. Implementing this in a way that makes a time domain calculation easily executable is the first objective.

2. The time and frequency domain equations are each other's counterpart in their respective domain; both are linear equations of motion. The results of both algorithms should therefore be the same. Verifying that the Cummins equation indeed produces similar results as the frequency domain is the second objective.

3. Implementing an algorithm that is able to identify force coefficients from measured and predicted motions will be the third objective. These coefficients can then be used to re-predict the motions, with the new and updated coefficients.

4. The ultimate identification is to be performed using field data, collected by the Acta Auriga while at sea. This data is not automatically suitable for the identification algorithm and should therefore be pre-processed. Processing the field data to usable format is the fourth objective.

5. From the processed field data, coefficients for the Cummins equation will be identified. Determining which coefficients are eligible for this and then finding appropriate values for them using the algorithm described above, will be the fifth objective.

6. To conclude, the motions will be re-predicted using the updated or added coefficients in the Cummins equations. The aim is that these re-predictions are of improvement accuracy, compared to the predictions made by Next Ocean. The performance of a prediction will be expressed by a correlation coefficient, quantifying the match between measured motions and predictions.

All research was performed using data of the Acta Auriga, a 93 metre long offshore supply vessel, build in 2018 and operated by Acta Marine.

1.4. Report Structure

This section shortly describes the structure of the report.

- Chapter 2: **Theory and Implementation** is concerned with describing the relevant theoretical background. The theory behind time domain modelling of floating objects is elaborated on. Also a short introduction to linear seakeeping in the frequency domain is provided. Procedures taken to implement the Cummins equation are described as well in this chapter.
- Chapter 3: **Results** elaborates on the obtained results corresponding to the different sub-objectives. Unexpected results are described and further investigations done into these results are described as well.
- Chapter 4: **Discussion and Conclusion** discusses the implication of the results presented in chapter 3 and conclusions regarding the research objectives are presented. Further research suggestions are provided in this chapter too.
- In the **appendices**, more graphs and plots are shown. These have not been placed in the main text since they are of less importance to the main lines of reasoning and to ensure readability.

2

Theory and Implementation

2.1. Introduction

In this chapter the theory used throughout the project will be described. The first section will describe linear seakeeping in general. Sections 2.2 and 2.3 will cover seakeeping modelling in frequency and time domain, respectively. The theory on time domain modelling is of prime importance for this project. The final two sections will cover the coefficient identification process and will elaborate on the implementation.

As any rigid body, a floating ship has six degrees of freedom (DOF's). Three are linear and three are rotational. These motions are usually defined with respect to the vessel's centre of gravity (COG). The DOF's are depicted in figure 2.1 and their symbols and respective numbers are shown in table 2.1.

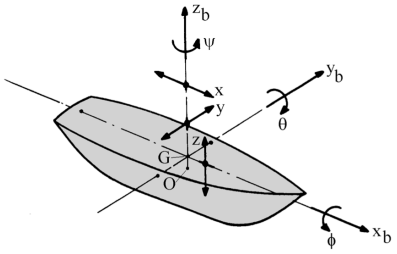

Figure 2.1: The six degrees of freedom depicted

DOF	Number	Symbol
Surge	1	x
Sway	2	y
Heave	3	z
Roll	4	θ
Pitch	5	ϕ
Yaw	6	ψ

Table 2.1: The symbols of the DOF's

The motion past/around the x, y and z axes can be modelled in both the time and frequency domain. Each of these approaches has its own advantages. Before these two are described in more detail, a general section on linear seakeeping will be presented.

2.1.1. General Linear Seakeeping

In linear seakeeping, a number of assumptions are made when it comes to the forces involved. These forces consist of vessel mass related inertia forces, excitation forces, hydrodynamic reaction forces and hydrostatic forces. Excitation forces are the forces the water would apply to the vessel if it was not to move. The reaction forces are the forces the vessel applies to the water it is floating in. These forces arise due to the motion of the vessel and are considered to be from a moving vessel in flat water. Hydrostatic forces are forces that originate from a body being submerged in water according to Archimedes principle. One of the main assumptions in linear seakeeping is that the excitation forces are independent of the reaction forces. Furthermore, it is assumed that the excitation forces scale linearly with wave height and that the reaction and hydrostatic forces scale linearly with vessel motion amplitude. Any deviations from these assumptions would mean that one is no longer using linear seakeeping theory.

With floating objects, deviations from linear seakeeping might thus originate from many sources. The degree to which the linear assumptions are reasonable depends, amongst others, on the vessel's hull shape, the motion amplitudes and on wave height and form. Although linear seakeeping theory provides satisfactory results on many occasions, there are also applications where a deviation from this theory is needed. This thesis is an effort to investigate the possibilities of adding non linear components to the equations of motion.

The Equation of Motion

The seakeeping of vessels can be modelled by solving the equations of motion, with the wave excitation force as an input. First the linear equations of motions will be described. The position of the ship under consideration will be described by the vector $\vec{x}$. It's first and second time derivative, $\dot{\vec{x}}$ & $\ddot{\vec{x}}$, will then describe the ship's velocity and accelerations respectively. When the full position of the vessel is considered, $\vec{x}$ has six elements; the three translational positions as well as the three angular positions. Starting with Newton's second law, the equations of motion can be constructed.

$$\vec{F} = \frac{d([M]\dot{\vec{x}})}{dt} = \vec{F}_{Wave\,Excitation} + \vec{F}_{Reaction} + \vec{F}_{Hydrostatic} \tag{2.1}$$

The hydrostatic forces are a function of only the position of the vessel. The reaction forces are induced by the vessel's motion, and are therefore a function of its velocity and acceleration. This suggests an equation of the following form:

$$[M] \cdot \ddot{\vec{x}} = -[A] \cdot \ddot{\vec{x}} - [B] \cdot \dot{\vec{x}} - [C] \cdot \vec{x} + \vec{F}_{Wave\,Excitation} \tag{2.2}$$

The minus signs are convention. The above equation is a vector equation, therefore the coefficients $[M]$, $[A]$, $[B]$ and $[C]$ will be matrices of size 6 by 6. Coefficients in the $[A]$ matrix are associated with the acceleration of the vessel and can therefore be seen as coefficients of inertial forces and moments; the matrix is referred to as the added mass matrix. The matrix $[B]$ is associated with velocities and is therefore referred to as the damping matrix. Coefficients in the $[C]$ matrix act as spring constants; they are associated with the position of the vessel and it will be referred to as the restoring matrix. The equations of motion for floating objects thus naturally take the form of a damped mass spring system.

Coupling Between Degrees of Freedom

As shown in the previous section, the full equation of motion has its force coefficients placed in matrices. In the most general case of a floating object, all positions in the matrices have nonzero values. The off diagonal terms in the matrices are referred to as coupling terms; they couple motions and positions in one direction to forces in another direction. In a randomly shaped floating object, a coupling between a motion or position along each axis is coupled to forces in all other directions. When axes of symmetry are present in the vessel's underwater hull shape, couplings between certain DOF's are lost. Ships tend to be symmetrical in the x-z plane; port-starboard symmetry. This removes half of the couplings and creates two sets of coupled motions; surge-heave-pitch and sway-roll-yaw. No coupling between these sets is present. These two sets of motions are called symmetric and anti-symmetric motions respectively. Two points that are in opposite positions with respect to the x-z plane will remain at a fixed distance from this plane when symmetric motions occur, this distance changes for anti-symmetric motions.

For general ships, those symmetric in the x-z plane, the $[A]$ matrix from equation 2.2 has the following structure, showing the two sets of couplings.

$$A = \begin{bmatrix} a_{1,1} & 0 & a_{1,3} & 0 & a_{1,5} & 0 \\ 0 & a_{2,2} & 0 & a_{2,4} & 0 & a_{2,6} \\ a_{3,1} & 0 & a_{3,3} & 0 & a_{3,5} & 0 \\ 0 & a_{4,2} & 0 & a_{4,4} & 0 & a_{4,6} \\ a_{5,1} & 0 & a_{5,3} & 0 & a_{5,5} & 0 \\ 0 & a_{6,2} & 0 & a_{6,4} & 0 & a_{6,6} \end{bmatrix}$$

The damping matrix has the same structure. The mass matrix $[M]$ and restoring matrix $[C]$ have deviating structures. The mass matrix will be considered a diagonal matrix in this project:

$$M = \begin{bmatrix} m & 0 & 0 & 0 & 0 & 0 \\ 0 & m & 0 & 0 & 0 & 0 \\ 0 & 0 & m & 0 & 0 & 0 \\ 0 & 0 & 0 & I_{x,x} & 0 & 0 \\ 0 & 0 & 0 & 0 & I_{y,y} & 0 \\ 0 & 0 & 0 & 0 & 0 & I_{y,y} \end{bmatrix}$$

Note that rotational moment of inertia around the z-axis is set to be equal to that of the moment of inertia around the y-axis. This is because these quantities differ only ever so slightly. The restoring matrix $[C]$ will have the following entries:

$$C = \begin{bmatrix} 0 & 0 & 0 & 0 & 0 & 0 \\ 0 & 0 & 0 & 0 & 0 & 0 \\ 0 & 0 & C_{3,3} & 0 & C_{3,5} & 0 \\ 0 & 0 & 0 & C_{4,4} & 0 & 0 \\ 0 & 0 & C_{5,3} & 0 & C_{5,5} & 0 \\ 0 & 0 & 0 & 0 & 0 & 0 \end{bmatrix}$$

Considering the last matrix, a second distinction between motions can be made. Motions that have a restoring force (heave, roll and pitch) and motions that do not (surge, sway and yaw). This distinction turns out to be of great importance for modelling in the time domain. Absence or presence of restoring forces may be intuitively understood. A displacement in the surge direction for example will not counteract itself; a ship that is moved a metre in its x direction will have no tendency to return to its initial position. A displacement of a metre in the heave direction however, will result in a large force towards the position the vessel came from.

The elements in the mass matrix $[M]$ are determined during the design of the vessel, and they consist of the mass of the vessel and the moments of inertia. The other hydrodynamic coefficients: $[A]$, $[B]$ and $[C]$, along with the excitation force coefficients can be determined using diffraction analysis software. Diffraction analysis is based on potential flow theory, which does not take the viscosity of the fluid into consideration. Therefore, the damping from the aforementioned $[B]$ matrix originates only from waves being radiated from the moving vessel, thereby taking energy from the moving ship. Furthermore, for a vessel at zero speed, it holds that the coefficient matrices are symmetrical; $a_{i,j} = a_{j,i}$, this holds for the matrices $[M]$, $[B]$ and $[C]$ as well.

Frequency Dependent Coefficient Matrices
To conclude this introduction on linear seakeeping, it is important to mention that some of the coefficients in the mass spring damper equation, Eq. 2.2, for floating objects are frequency dependent. This means that the values in the matrices $[A]$ and $[B]$ are only valid for a single harmonic motion frequency. Matrices $[A]$ and $[B]$ are therefore to be calculated on a predetermined set of frequencies, using the diffraction software. The restoring matrix is concerned with static forces, and is therefore frequency independent. The wave excitation force is dependent on both the wave frequency and the direction of the incoming waves. These first order wave forces are obtained by multiplying the wave height of a single wave component, with its own frequency and direction, by the corresponding excitation force coefficient, also determined by the diffraction code. In this document, these matrices and excitation coefficients are together referred to as the hydrodynamic database of the ship.

The ship model can thus more accurately be seen as a frequency dependent damped mass spring system. In time domain modelling, there can therefore not be one single value for each position in the hydrodynamic matrices. How to deal with this frequency dependency in the time domain is described in more detail in the section on time domain modelling.

In this project, the hydrodynamic coefficients, the mass matrix and the excitation coefficients, i.e. the hydrodynamic database, are considered to be known as these are often available for modern vessels.

2.2. Frequency Domain Model

The fact that the hydrodynamical coefficients are frequency dependent makes a model in the frequency domain an alluring option; when motion at a single frequency is considered, the coefficient matrices will be constant. When excitations are considered to be harmonic, the frequency domain equation of motion can be yet more insightful. Due to the linearity of the model, a sinusoidal excitation will also result in a sinusoidal motion response with the same frequency, but with its own amplitude and phase. By using Euler's identity to write sinusoids as complex exponentials, the frequency domain counterpart of Eq. 2.2 for a single frequency can be written as follows:

$$-\omega^2\left([M]+[A]\right)\cdot\vec{a}\,e^{-i\omega t+\phi}+\omega[B]\vec{a}\,e^{-i\omega t+\phi}+[C]\vec{a}\,e^{-i\omega t+\phi}=\vec{F}_o\zeta_a e^{-i\omega t} \tag{2.3}$$

Here, on the right hand side, the excitation is written as $\vec{F}_o\zeta_a e^{-i\omega t}$, where $\vec{F}_o$ are the 6 force coefficients in $[N/m]$ or $[Nm/m]$, and ζ_a is the wave amplitude. $e^{-i\omega t}$ is a harmonic function with frequency ω. On the left hand side, $\vec{a}e^{-i\omega t+\phi}$ represents a harmonic motion response with a certain amplitude vector $\vec{a}$ and a phase ϕ with respect to the excitation force. Furthermore, note that the time derivatives, the velocity and accelerations, are represented by the factors $i\omega$ and $-\omega^2$ respectively. [13], [6].

A Motion Transfer Function

As with many linear models in the frequency domain, a transfer function can be determined. In seakeeping theory it is common to define this transfer function between the wave amplitude and the motion amplitude. This transfer function is often referred to as the RAO; Response Amplitude Operator. The RAO can be calculated from Eq. 2.3. Note however that Eq. 2.3 is written for a single wave frequency and direction. The RAO is a function of both these quantities:

$$\text{RAO}(\omega,\mu)=\frac{\vec{a}}{\zeta_a}=\frac{\vec{F}_o(\omega,\mu)}{-\omega^2\left([M]+[A]\right)+i\omega[B]+[C]} \tag{2.4}$$

The division of by the sum of matrices is done by multiplication with the inverse of this sum of matrices. By calculating the RAO like this, each frequency and wave direction will yield a vector of six elements, where each element represents the transfer function value of a single degree of freedom. Calculating the RAO like a vector, as described by Eq. 2.4, is done to incorporate the couplings between the different degrees of freedom. All hydrodynamic coefficients are real valued numbers, the excitation force coefficients however, are complex valued. Therefore the RAO is also complex valued, having both an absolute value and a phase. The absolute value indicating the motion amplitude, for a given wave frequency and direction, per meter wave height. The phase of the RAO indicates the phase difference between the incoming wave and the considered motion.

In linear modeling of seakeeping, the RAO is often used to determine the vessel motion response in a given wave field consisting of multiple waves with varying frequency. The superposition principle is extensively used in modelling vessel motions using the RAO, as a ship in a realistic wave field experiences waves with multiple frequencies, coming from multiple directions. Using Fourier series, a wave realisation can be written as a sum of harmonic components. Each of these components has an effect on the vessel motion that can be determined using the RAO. By adding the responses to the individual wave components, the response to a spectral wave input can be determined.

Opposed to this deterministic motion calculation, the RAO can also be used in a more statistical way, as was introduced as an often used method to asses probabilities of exceedance, in the introduction. Given a wave spectrum, a motion spectrum can be calculated using the RAO:

$$S_R=|\text{RAO}|^2\cdot\zeta_S \tag{2.5}$$

Where S_R is the response spectrum and ζ_S the wave spectrum. Note that the absolute value and square of the RAO are for a single degree of freedom, i.e. only a single element of the vector that is the result of the RAO calculation described by equation 2.4 is used. Using the response spectrum, statistical predictions can be made for the motion that will be encountered in a given sea state. One could for example determine the chance of exceeding a given motion amplitude during a given time, in a given sea state. Spectra used in these calculations only contain information on how the wave and motion

energy is distributed over frequencies and directions. The stochasticity arises form the fact that the phases of the wave components are assumed to be distributed randomly, with no dependency on the wave frequency or direction. It is worth mentioning that the same line of reasoning can be used to come up with transfer functions between the wave height and velocities or accelerations. Velocity or acceleration spectra can then be calculated, when the limiting criterion is not a position, but a velocity or acceleration instead. In this project however, the focus lies on deterministic prediction of positions.

The frequency model is only applicable for linear modelling. This stems from the fact that the RAO implies a fixed ratio between the wave amplitude and the resulting response. When non linearities, of which there might be multiple, come into play, this assumption no longer holds. A strongly flared hull shape will for example give rise to a position dependent restoring heave coefficient. If the waves double in height, the motions subsequently grow larger. These larger motions will then lead to restoring forces that grow non linearly. Therefore, the steady state motion amplitude will not double. Modelling motions while incorporating any possible non linear effect, cannot be done using the just described frequency domain, it can however be done in the time domain.

2.3. Time Domain Model

As described in the introduction of this chapter, the frequency dependent coefficients in the equations of motion, Eq. 2.3, prevents straightforwardly solving for the motions in the time domain. Using a differential equation solver, it is not trivial which coefficient to ultimately use in the equations. The frequency dependency introduces what is sometimes called 'the memory effect' for the reaction forces. This implies that the reaction forces do not only depend on the current velocity and acceleration, but also on motions in the past. If a floating object moves in still water, the movement causes the surrounding water to move with it. If the object was to stop or change its motion abruptly, the water surrounding it would still be in movement due to the earlier motion of the object and would thereby still apply forces and momtents on the vessel. This illustrates why motions from the past have an effect on current reaction forces.

Cummins formulated an equation that takes these past motions into account. His line of reasoning is based on the use of an impulse response function to formulate the reaction forces. According to Cummins, back in 1962; 'the basic tool which will be used in this study is an elementary one, widely used in other fields and well known to all engineers: the impulse response function. It is difficult to understand its neglect in our field.' Many papers have since been written on how to implement the equation conveniently, yet still today in many practical applications the frequency domain model, including its stringent demand for linearity, is often the method of choice. Supposedly, this is at least partly due to the relative ease of implementation and the often satisfactory results, also in statistical wave response predictions. As described, implementing nonlinearities forces one away from the use of the frequency domain model.

Cummins Equation

Cummins' line of reasoning is frequently described in papers published after his classical work in 1962. His original paper being much more elaborate on the background and showing the correctness of the approach, only his main line of reasoning will be described here.

Suppose a vessel floating motionless in still water. If the vessel were to be instantly moved in one direction, with a constant velocity V, during a time Δt. The resulting displacement would be as follows:

$$\Delta x = V \cdot \Delta t \tag{2.6}$$

This movement will cause the water surrounding the ship to move. If the fluid is regarded non viscous and the fluid motions are non rotational, the fluid motions can be described using a velocity potential function,Φ, which is proportional to the velocity V.

$$\Phi = V \cdot \Psi \qquad \text{for } t_0 < t < t_0 + \Delta t \tag{2.7}$$

Here, Ψ is a normalised velocity potential. This potential is valid during the displacement; $t_0 < t < t_0 + \Delta t$. After this time, the fluid is still moving, meaning that Φ does not become zero right after $t_0 + \Delta t$. During this later time, the velocity potential is assumed to be proportional to the displacement Δx:

$$\Phi = \Delta x \cdot \Theta = V \cdot \Delta t \cdot \Theta \qquad \text{for } t > t_0 + \Delta t \tag{2.8}$$

Where Θ, too, is a normalised velocity potential, concerned with fluid motions at times past $t_0 + \Delta t$, whereas Ψ is concerned with fluid motions between t_0 and $t_0 + \Delta t$.

Consider now a vessel that has been moving in all six degrees of freedom for a longer period of time. The velocity potential at a given moment is then dependent on the current displacements (as descirbed by Eq. 2.7), but also on the previous displacements (as described by Eq. 2.8). Suppose that this longer period of time is divided in n sections with length Δt, during each of which the vessel moves with a different but constant velocity V. At a given moment t, the total potential, Φ,can then be described as:

$$\Phi(t) = \sum_{j=1}^{6} [\underbrace{V_{j,n} \cdot \Psi_j}_{\substack{\text{Current velocities;} \\ \text{Eq. 2.7}}} + \sum_{k=1}^{n} \underbrace{\Theta_j(t_{n-k}, t_{n-k} + \Delta t) \cdot V_j(t_{n-k}, t_{n-k} + \Delta t) \cdot \Delta t}_{\text{Past velocities; Eq. 2.8}}]$$

Note that in contrast to equations 2.6, 2.7 and 2.8, motions in all 6 degrees of freedom are considered. When Δt goes to zero, the second summation becomes an integral. According to Journée [12]:

$$\Phi(t) = \sum_{j=1}^{6} V_j(t) \cdot \Psi_j + \int_{-\infty}^{t} \Theta_j(t-\tau) V_j(\tau) d\tau \tag{2.9}$$

This velocity potential can then be used to come up with the pressure in the fluid, p, using the Bernoulli equation:

$$\mathrm{p} = -\rho \cdot \frac{\partial \Phi}{\partial t}$$

Where ρ is the fluid mass density. In order to determine the forces the vessel applies to the fluid, F, the pressure is to be integrated over the average wetted body surface of the vessel, S:

$$F_i = \int \int_S \rho \frac{\partial \Phi}{\partial t} \cdot n_i dS \tag{2.10}$$

Here, n_i is the generalised directional cosine function where $i = 1$ to 6, which accounts for the orientation of the surface with respect to the direction of the force under consideration. Note that forces and moments in all six directions can be obtained in this manner. By combining Eq. 2.10 and Eq. 2.9, the following expression for the hydrodynamic reaction forces is obtained:

$$F_i = \rho \sum_{j=1}^{6} \dot{V}_j(t) \int \int_S \Psi_j \cdot n_i dS + \int_{-\infty}^{t} \left(\int \int_S \frac{\partial \Theta_j(t-\tau)}{\partial t} \cdot n_i dS \right) V_j(\tau) d\tau \tag{2.11}$$

When defining:

$$A_{\infty\, i,j} = \rho \int \int_S \Psi_j \cdot n_i dS \tag{2.12}$$

and:

$$\kappa_{i,j}(t) = \rho \int \int_S \frac{\partial \Theta_j}{\partial t} \cdot n_i dS \tag{2.13}$$

Using Eq. 2.12 and Eq. 2.13, the expression for the reaction forces, Eq. 2.11, simplifies to:

$$F_i = \sum_{j=1}^{6} \dot{V}_j A_{\infty\, i,j} + \int_{-\infty}^{t} \kappa_{i,j}(t-\tau) V_j(\tau) d\tau$$

Combining these reaction forces with body mass related inertia forces and the restoring forces, the equation of motion in the time domain, without frequency dependent coefficients, is obtained. These equations are known as the Cummins equations [3]:

$$\sum_{j=1}^{6} \left(A_{\infty\, i,j} + M_{i,j}\right) \ddot{x}_j(t) + \int_{-\infty}^{t} \kappa_{i,j}(t-\tau)\dot{x}_j(\tau)d\tau + C_{i,j}x_j = F_{\text{excitation } i} \tag{2.14}$$

for $i = 1$ to 6. For $i = 4, 5, 6$, equation 2.14 applies to moments in stead of forces. To the Cummins equation, extra forces can be added as deemed necessary. In this project, non linear damping forces were added, but also forces imposed by mooring systems could be accounted for, as well as other nonlinear contributions.

Cummins and the Hydrodynamic Database
In the previous section, the equations of motion for a floating object in the time domain were described; the Cummins equations. The hydrostatic forces coefficients can be obtained from the water plane area and the tranverse and longitudinal metacentric height, GM and GM_L respectively. The excitation forces can be obtained from refraction calculations. Two main terms of this equation are however yet unknown; $A_{i,j}$ & $B_{i,j}$, for $i = 1$ to 6 & $j = 1$ to 6. Finding the velocity potentials to be able to solve the equations of motions is highly complex [12]. Ogilvie formulated relations to tie these unknowns to the more easily obtainable frequency dependent force coefficients [17].

The main idea of Ogilvie's work is to compare the Cummins equation with the frequency domain equation of motion for a single frequency; both these equations should both give the same result. By considering a simple harmonic motion in the Cummins equation and rewriting its components, a termwise comparison between the two equations of motion, results in the following relations:

$$\kappa_{i,j}(\tau) = \frac{\pi}{2}\int_0^{\infty} b_{i,j}(\omega) \cdot \cos(\omega\tau)d\omega \tag{2.15}$$

and

$$A_{\infty\, i,j} = a_{i,j}(\omega) + \frac{1}{\omega}\int_0^{\infty} B_{i,j}(\tau)\sin(\omega\tau)d\tau \tag{2.16}$$

$\kappa_{i,j}$ is known as the retardation function, and can be seen as the impulse response function that takes the velocity as an input and gives a reaction force as an output. τ is the retardation time; the retardation function will thus be a function of time. $b_{i,j}(\omega)$ are the frequency dependent damping force coefficients in the hydrodynamic database. $A_{\infty\, i,j}$ is known as the infinite frequency added mass. In equation 2.16, $a_{i,j}$ denotes the frequency dependent added mass, described in section 2.1.1. In the determination of $A_{\infty\, i,j}$ it is ambiguous what omega to use. Theoretically, the choice of frequency does not affect $A_{\infty\, i,j}$. When hydrodynamic coefficients are available up to very high frequency, the contribution of the integral vanishes and the high frequency value of the coefficient dominates. In practical cases, the maximum frequency at which the hydrodynamical data is known is not high enough to take the maximum frequency value of the added mass. In the implementation it could clearly be seen that the added mass converges to a constant value, see figure 2.4. Only for low frequencies, values produced by Eq.2.16 varied slightly. Higher frequencies produce more stable results.

Solving the Convolution Integral
The Cummins equation, Eq. 2.14, contains a convolution integral. In an irregular wavefield, the vessel motions are continuously changing, therefore the motion history on which the reaction forces are based will in general be unique at any given moment in time. This implies that for every timestep taken in solving the equations of motion, the convolution integral is to be calculated anew. Point of interest has been to find methods to compute this convolution in an efficient manner. A comparison between multiple methods has been made by Armesto et al. [11]. Armesto evaluated three different methods; direct integration, approximation by state space and approximation by Prony coefficients and yet another method was used by Hasmi[1]. Methods other than direct integration have been developed to save computational time. Armesto compared the methods regarding their results and computation time needed and concluded that all three methods gave similar results. Differences were found in sensitivity;

state space and Prony coefficients showed to be sensitive to the way the frequency dependent hydrodynamic coefficients were prepared. Results obtained via direct integration showed a dependency on the chosen timestep for the determination of the retardation function. This was more pronounced in frequencies near resonance.

As described, the alternatives to direct integration were motivated by a possible gain in computation time. According to Armesto, time could be saved when considering single degree of freedom motions, meaning that coupling between DOF's in not accounted for. However, when considering coupled DOF's, the alternative methods investigated by Armesto took longer than the direct integration approach. This, combined with possible artifacts due to the fact that the convolution integral is approximated when using state space or Prony's method, lead to Armesto's conclusion that the direct integration method is to be preferred. In this project, the direct integration method is therefore used to solve the Cummins equation.

Retardation Based on Added Mass

The retardation function can be seen as the impulse response function that takes the past velocities as an input and delivers reaction forces as an output. The Ogilvie relations, equations 2.15 and 2.16, lead to the frequency dependent hydrodynamic damping coefficients as the base of the retardation function and the infinite frequency added mass. The hydrodynamic reaction forces are however a result of both the velocity and acceleration of the vessel, this implies that the retardation function could also be based on the frequency dependent added mass.

When again regarding motion with a single frequency ω, the velocity $v(t)$ can be described as a sinusoidal function in the complex notation, with a frequency of ω as well:

$$v(t) = V_a e^{i\omega t} \tag{2.17}$$

Where V_a is the amplitude of the velocity. The acceleration of that same motion, $\dot{v}$, can then be described as:

$$\dot{v} = i\omega V_a e^{i\omega t} \tag{2.18}$$

The retardation function can be seen as the impulse response function relating the velocity to the hydrodynamic reaction force. This force will partly be in phase with the velocity, Eq. 2.17, and partly with the acceleration, Eq.2.18. In the frequency domain, where the response of a system is the multiplication of the transfer function and the input, the transfer function, $H(\omega)$ could thus be written as follows:

$$H(\omega) = i\omega\alpha + \beta$$

This can be motivated by looking at the resulting hydrodynamic reaction force, F_{HR}:

$$F_{HR}(\omega) = H(\omega) \cdot V(\omega) = \underbrace{\alpha i\omega V(\omega)}_{\substack{\text{in phase}\\ \text{with}\\ \text{acceleration}}} + \underbrace{\beta V(\omega)}_{\substack{\text{in phase}\\ \text{with}\\ \text{Velocity}}} \tag{2.19}$$

Here, α represents the part of the hydrodynamic reaction force in phase with acceleration and can therefore be regarded as the added mass for frequency ω, β is the part in phase with velocity and can therefore be seen as the damping. $V(\omega)$ represents the velocity, expressed in the frequency domain. The real part of the transfer function, H_r, is β and the imaginary part, H_i, is $\omega\alpha$.

In general, the impulse response function, the time domain equivalent of the transfer function, can be obtained by taking the inverse Fourier transform of the transfer function, for causal systems it holds that using either only the real or only the complex part suffices, resulting in two possibilities for obtaining the impulse response function:

$$\text{IRF}(t) = \frac{\pi}{2}\int_0^\infty H_r(\omega)\cos(\omega t)d\omega = -\frac{\pi}{2}\int_0^\infty H_i(\omega)\sin(\omega t)d\omega \tag{2.20}$$

Here, IRF stand for Inpulse Response Function. From equation 2.20 it can be seen that the retardation function can also be based on the frequency dependent added mass coefficients, i.e. $H_i(\omega)$ in the right

most part of Eq.2.20. Retardation based on damping is however to be preferred, since the damping curve decays faster with increasing frequency. The integration in Eq.2.20 is to be done to infinite frequency, after the coefficients in the hydrodynamic database ($H_r(\omega)$ or $H_i(\omega)$ in Eq.2.20) have become zero, further integration is senseless. Using a damping based retardation function thus means that data to lower maximum frequency suffices. This is particularly important since the vessel response to excitation forces has died out at much lower frequencies, meaning that the high frequency values of the coefficients are often not available in databases not meant to use for time domain simulations. To conclude, the higher the maximum frequency at which the coefficients in the hydrodynamic database are to be calculated, the smaller the panels or strips in the potential code need to be. Given a certain maximum frequency, time domain prediction using a damping based retardation function will thus be more accurate.

2.4. Coefficient Identification

A sub objective of this thesis is the identification of force coefficients from field data. Identification can be either used to find new coefficients of forces that are not yet present in the earlier shown Cummins equation (i.e. the added roll damping force), or already existing force coefficients might be updated to a better performing value. The already existing force coefficients mentioned here can be any entry in the $[M]$, $[A_\infty]$ or $[C]$ matrix in the Cummins equation, Eq. 2.14.

In the identification process, the equations of motion are used. Both the force predictions, made by Next Ocean and the motion measurements are of importance in the coefficient identification. Using these predictions and measurements, all terms in the equations of motion can be calculated, for every timestep separately. Inertia, damping and restoring forces will be determined from the motion measurements using their respective definition in the Cummins equation. Since errors will be present in the predicted excitation forces and the equation of motion is not a perfect model, there will be a discrepancy between the left hand side of the equations of motion, where the forces based on motion measurements are placed, and the right hand side, where the force predictions are located. This discrepancy is referred to as the force-or moment residual in the remainder of this thesis. When considering an uncoupled motion, the residual is defined as follows:

$$\vec{F}_{residual} = \vec{F}_{excitation} - \left([M + A_\infty] \cdot \ddot{\vec{x}}(t) + \int_0^t [K(t-\tau)\dot{\vec{x}}(\tau)d\tau + [C] \cdot \vec{x}(t) \right) \tag{2.21}$$

When the motions are coupled, as is always the case in coefficient identification using field data, the matrices in the above equation, $[M]$, $[A_\infty]$, $[K]$ and $[C]$ have off diagonal entries. The main idea behind the identification process is that the force residuals still contain usable information. When all forces relevant for the motion are present in the equations of motion, and the description or prediction of these forces is performed accurately (for example the right function form to calculate a certain force is used and the coefficients used are correct), there is no reason expect information in the force residuals. This means that the modeling of a purely linear degree of freedom, with accurate force coefficients and an unbiased force prediction should in theory not be improved by force coefficient identification.

For the roll motion a founded suspicion for a relatively large importance of friction damping is present. The cross section of a vessel typically having a relatively round shape, leads almost to the absence of potential damping. The potential code however, only determines this potential damping, thereby neglecting the relatively large friction damping. The absence of this friction force in the equations of motion motivates the suspicion that information is still available from the force residuals. The friction force will be described using a third order polynomial:

$$F_{\text{friction }44}(t) = \alpha \cdot \dot{x}(t) + \beta \cdot |\dot{x}(t)|\dot{x}(t) + \gamma \cdot \dot{x}^3(t) \tag{2.22}$$

Friction force is often presented as being a quadratic function of velocity, a linear and cubic dependency may be present as well. Therefore a third order polynomial was assumed. For other degrees of freedom, no such absence of a force in equations of motions is to be expected. Some of the already present forces may however not have highly accurate force coefficients. Radii of gyration, associated with inertia moments, are for example often estimated from rules of thumb, instead of calculated from

the mass distribution. Furthermore, mass and radii of gyration may change significantly depending on load conditions. Such uncertain coefficients may also be determined with more accuracy by identification from field data.

For the identification, only the coupled equations of motion can be used, as the measured motions are from a real vessel that cannot move without coupling between the degrees of freedom. This means that all coupling forces are present. Generally, the equations of motion must therefore be regarded as a system of equations. When no cross terms are to be identified however, each of the six equations in the system of equations can be regarded separately when performing parameter identification. The fitting through the force and moment residuals, what the identification in this project ultimately entails, can in this case be performed using multiple linear regression analysis. In the more general case, where one would also be able to fit coupling coefficients, i.e. the off diagonal entries in the matrices $[M]$, $[A_\infty]$ and $[C]$, the equations become interconnected. Six dependent variables; the residual forces and moments, are described by one fixed group of predictor variables; acceleration, velocity and position in all degrees of freedom. Strictly speaking, two groups of dependent and independent variables could be separated, as no couplings are present between surge, heave and pitch on the one hand and sway, roll and yaw on the other. In this more general case, multivariate regression analysis is to be used.

Multivariate regression analysis works best when the predictor variables are orthogonal to each other, meaning that they are uncorrelated to each other. When using position, velocity and acceleration as predictor variables, this is not the case. When a single frequency motion is regarded, position and its derivatives are highly correlated. When a spectrum is however considered, this correlation reduces. The wider the spectrum becomes, the less correlated position and its time derivatives become. More severe sea states have, besides more nonlinear roll damping, a wider spectrum, making motion records of rough periods more suitable for identification. The RAO of a vessel is however a limiting factor, since this transfer function functions as a filter; only transmitting a range of frequencies to the actual vessel motions. This is especially true for the roll motion, having a very narrow peak in the RAO. In that regard, roll motions is the least suitable degree of freedom to perform coefficient identification on, when using multivariate regression analysis.

2.5. Cummins Implementation

The following section will describe the procedures used to obtain the retardation functions and the infinite frequency added masses needed for time domain modelling and is mainly concerned with practicalities relevant for determining the retardation and added mass.

2.5.1. The Retardation Function

Section 2.3 described the origin of the retardation function κ, and motivated the use of the damping coefficients to determine it. As seen in Eq. 2.15, the retardation function will be a function of time, and it can be obtained by integrating the damping curve, multiplied with a cosine, over all frequencies. In theory, the damping for any degree of freedom is to diminish with increasing frequency, making an upper limit until which to integrate arise naturally. The decrease of the damping curve is typically (by far) not advanced enough to assume zero damping at frequencies past the maximum frequency in the hydrodynamic database. Nonzero high frequency data is of large importance to the performance of the time domain code. This can be understood by considering Eq. 2.15; for low values of τ, the retardation function is closely related to the area under the damping curve. Ignoring the high frequency tail has therefore a significant effect on the amount of damping. This is elaborated on on page 20.

Obtaining stable and trustworthy results with the time domain code is therefore only possible when the high frequency tail of the damping curve is present. Fitting a tail to the curve in the frequency domain is therefore of vital importance for good time domain predictions. To fit a tail to the curve, the damping must be well past its highest point at the maximum frequency, otherwise the shape of the downward slope is not yet developed. Multiple functions can be used to describe the tail up to high frequencies, such as a $1/\omega^n$ or $e^{-\alpha\omega}$. Since the exact shape of the high frequency tail is not known, it is difficult to develop a clear preference for any of the possibilities and both base shapes produce very similar results. Armesto used the fact that an expression for the integral to infinite frequency for a

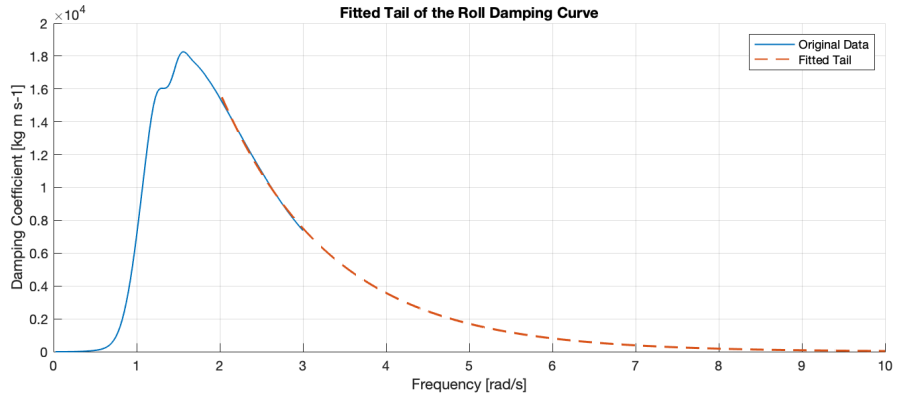

Figure 2.2: Roll damping in the hydrodynamic database, and an exponential tail fitted to the high frequency part of the curve.

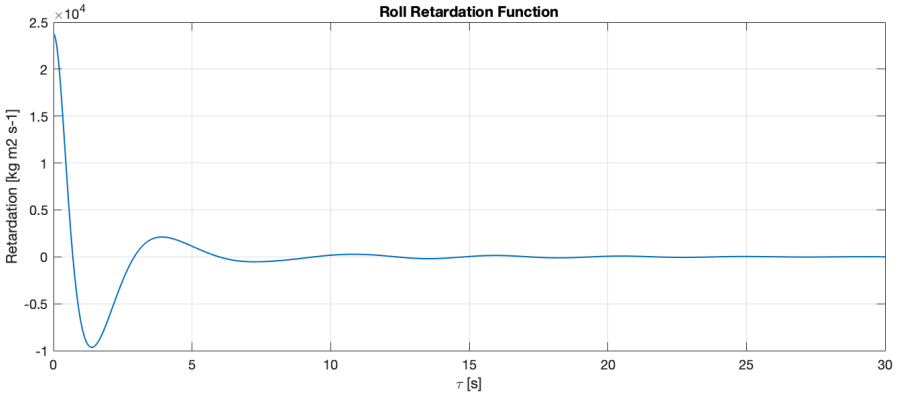

Figure 2.3: Roll retardation function.

cosine multiplied with an exponential tail is available. Using the same reasoning, the results presented in this thesis are also produced with an exponential tail fit for the damping curve. Figure 2.2 shows the damping for roll, as well as the fitted tail, figure 2.3 shows the corresponding retardation function.

2.5.2. Infinite Frequency Added Mass

From the retardation function, the infinite frequency added mass can be determined, which is used in the Cummins equation. The infinite frequency added mass is calculated using Eq. 2.16. Theoretically, the choice of ω in equation 2.16 is of no importance as the same A_∞ should be obtained for each choice of ω. Figure 2.4 shows the infinite frequency added mass calculated for different ω. Also, the frequency dependent added mass curve, $a_{4,4}(\omega)$ is shown, which makes a sensibility check of the obtained infinite frequency added mass possible. The dependence on the choice of ω indeed seems to be almost non existent. Some other degrees of freedom do show some oscillations in A_∞ for lower values of ω, in practice A_∞ is determined with the highest available frequency.

2.5.3. Implementing the Retardation Convolution

Via the retardation function, past motions are incorporated in the equations of motion. This is done by convoluting the retardation functions with past velocities. The convolution integral was discretized using the trapezoidal rule, as described by equation 2.23. In the Cummins equation, Eq. 2.14, the integration boundaries are $-\infty$ and t. However, the influence of past motions diminishes with time and can be neglected when further back in time than a certain t^*. The integration boundaries will then be from $t - t^*$ to t. Suitable values for t^* are suggested by Journée [12]. In this project, the maximum value of t^* is however limited by the $\Delta\omega$ for which the coefficients in the hydrodynamical database are known. t^* was set to 30 seconds. By this time, the retardation functions have negligible values, implying that this choice of τ_{max} would not cut of significant portions of the retardation function. The choice of $\tau_{max} = 30$ is elaborated on on page 20. Armesto [11] suggests a change in variables, $s = t - \tau$, which

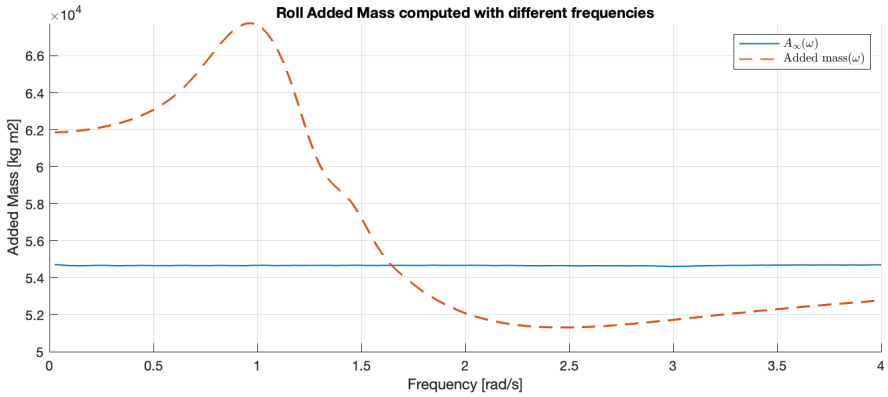

Figure 2.4: Roll infinite frequency added mass stabilises for higher frequencies, while showing very slight wiggles at lower frequencies.

will result in an integral from 0 to t^*, as shown in Eq.2.23. When regarding this equation for $s = 0$, the very first value of the retardation function, $K(0)$, is to be combined with the instantaneous velocity. This is however the velocity the ODE solver is trying to solve for. The retardation convolution integral can therefore be seen as composed of two parts. One is concerned with the instantaneous damping; a value that is treated as an ordinary damping in the function description used by the differential equation solver. The other part is concerned with velocities in the past, and while it changes every timestep, it is not combined with a to be solved for quantity (i.e. velocity, position). Looking at an individual timestep, the past velocity damping forces can thus be seen as external forces, added to the equation of motion, this is shown in equation 2.23.

$$\begin{aligned}\int_0^{t^*} K(s)\dot{x}(t-s)\mathrm{d}s &\approx \Delta t\left[\frac{K(0)\dot{x}(t)+K(t^*)\dot{x}(t-t^*)}{2}+\sum_{n=1}^{N-1}K(n\Delta t)\dot{x}(t-n\Delta t)\right] \\ &= \underbrace{\Delta t\frac{K(0)\dot{x}(t)}{2}}_{\text{Instantaneous damping}}+\underbrace{\Delta t\frac{K(t^*)\dot{x}(t-t^*)}{2}+\sum_{n=1}^{N-1}K(n\Delta t)\dot{x}(t-n\Delta t)}_{\text{Damping from past}}\end{aligned} \tag{2.23}$$

Where $N = {}^{t^*}/_{\Delta t}$. The equations of motion were solved using Matlab's ODE45 algorithm, which uses a combination of the 4th and 5th order Runge Kutta solving method. Note that in order to make the discretization in equation 2.23 work, the timestep taken by the differential equation solver is to be constant in size. No option to fix the timestep size is however available for ODE45. Fixing the timestep size was done by setting the initial timestep to the desired length, and by making only a single timestep. The outcome of this one timestep will then serve as the initial condition for the next timestep. This means that the ODE45 function was called N times to solve the equations of motion for the desired length of time. This approach differs from the way ODE45 is ordinarily used, where an end time is chosen and the algorithm decides on the optimal timestep size as it calculates the solution.

3

Results

This chapter describes the obtained results. It is divided in two main sections. The first section describes the results of the implementation of the Cummins equation. This section is roughly divided into four subsections; uncoupled motions with both monochromatic excitation and spectrum excitation and couples motions, also with both monochromatic and spectrum excitations. Some of these subsections are divided further to describe research into encountered problems. In this part of the chapter, extensive comparisons between results in the frequency domain and results from the linear Cummins equation are made. In figures showing this comparison, the abbreviation DS is often used, which stands for Domain Solution. The second section is concerned with the identification and re-prediction. Firstly, the procedure to make field data suitable for further usage is elaborated on, thereafter the identified coefficients are shown. To conclude this chapter, the re-predictions in the time domain are described.

3.1. Cummins Equation

The first section of the results will show the results obtained by the implementation of the Cummins equation. These time domain results will be compared to frequency domain results, as they should produce the same results. As described in the introduction, this comparison is made to gain confidence in the time domain simulations. These should be capable of reproducing the frequency domain results, before continuing to more complex simulations.

3.1.1. Uncoupled motion, Single Frequency Excitation

This section is divided in multiple subsections, as a number of difficulties arose when performing the first time domain simulations. Difficulties found here, are also present in the coupled motion simulations.

Zero Initial Position and Velocity

The first results will be of the most simple Cummins equation implementation; no coupling between the degrees of freedom, a monochromatic excitation and initial conditions for both position and velocity set to zero.

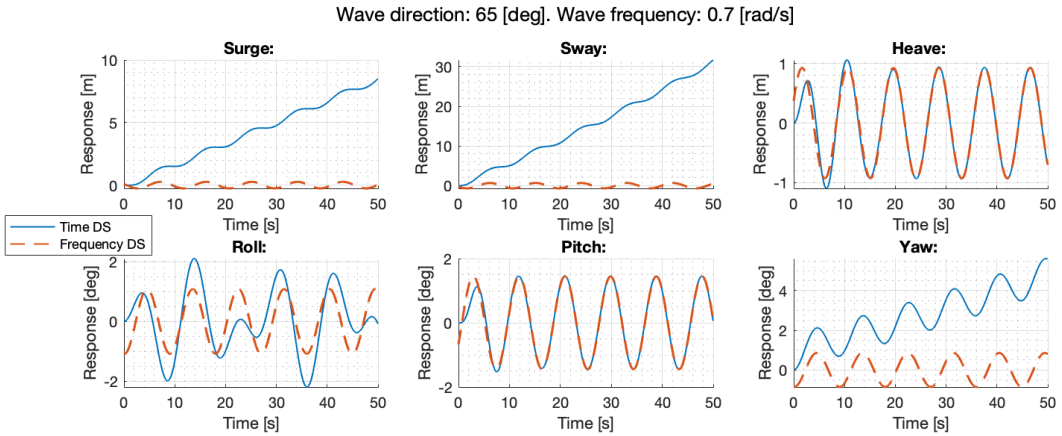

Figure 3.1: The most simple Cummins implementation results; uncoupled degrees of freedom, single frequency excitation and zero initial conditions. DS in the legend stands for Domain Simulation.

In this plot, that shows the motions of the vessel for 50 seconds, the transient response can clearly be distinguished in the early stages of the simulations. For heave and pitch, steady state is reached after about 2 oscillations. Surge, sway and yaw show a clear runaway behaviour. These degrees of freedom have in common that they do not have a restoring force. Errors in steady state position will therefore not result in a force that moves the vessel back to its original position.

Initially, the runaway behaviour was presumed to be initiated by the fact that the initial conditions were set to zero. This, combined with the fact that no past velocities were present to pre-load the retardation force, means that during the first moments of the simulation, there was no damping. The damping force in the Cummins equation is obtained by taking the convolution of the past velocities and the retardation function. This damping force should increase with time, slowing down the mean motion to find a new mean position around which it will oscillate.

Roll does not reach steady state during this simulation and performs a not harmonic motion. Here too, the lack of damping in the beginning of the simulation results in large differences between the results of the time-and frequency domain. Simulating for a longer period of time does not resolve the issues; the non-harmonic motion persists for periods longer than half an hour of simulated time, although the shape of the motion changes.

Matching Initial Conditions

The absence of a restoring force combined with a non-existent damping at the beginning of the simulation makes for runaway behaviour for surge sway and yaw. Roll does not converge to the frequency domain solution either. Adding damping to the beginning of the simulation was done by adding a section of artificial movement at times before the time domain simulation started. In the here described synthetic experiments, this was done using the frequency domain solutions. The frequency domain motions are created by using the RAO. Adding half a minute of negative time before $t_0 = 0$, creates motions and velocities in accordance with the frequency domain solutions. Besides introducing the possibility to start the simulation at a position and velocity matching that of the frequency domain solution, it also creates a means to use a proper damping force right from the start of the simulation. Next to as good as eliminating the transient period, adding past velocities can also mean the difference between reaching steady state or not. Figure 3.2 shows motions as response to a simple harmonic excitation force. Like heave and pitch, roll no longer shows transient behaviour and the response is nicely harmonic as well. Surge, sway and yaw still show the runaway behaviour, though much less pronounced when compared to the situation with initial conditions set to zero and no artificial past velocities.

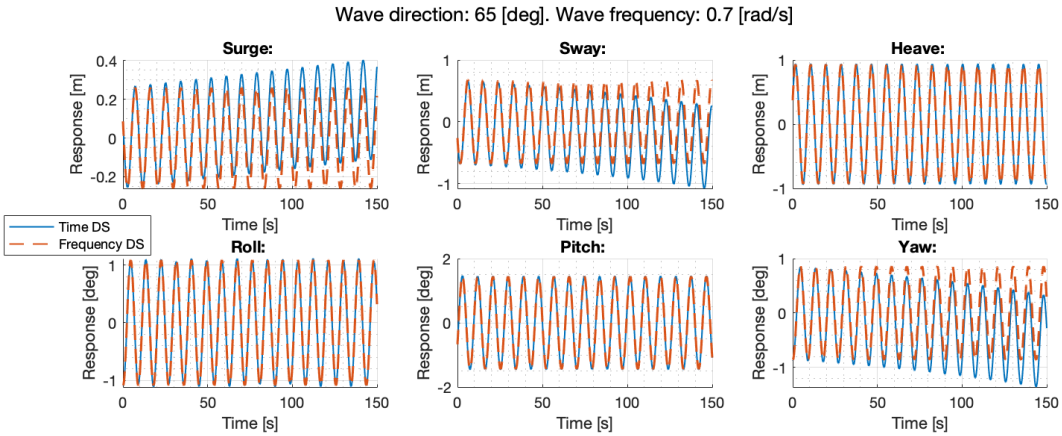

Figure 3.2: More elaborate initial conditions made for a closer match between time and frequency domain results. A past velocity is provided to load the damping and both initial position and velocity match the frequency domain solutions. The transient period is as good as gone.

It is important to mention that while in these synthetic data experiments an artificial velocity history is easily obtained, in the field such a velocity history is also available in the form of measured motions. The fact that these velocity histories turn out to have a crucial role in the performance of the time domain code, does therefore not mean that no role for this project's efforts are to be played in the field.

A Closer Look at Surge, Sway and Yaw

The running away behaviour of the surge, sway and yaw motion has been mentioned. The origin of this behaviour has not been discovered, but a closer study of these degrees of freedom has shown that surge, sway and yaw turn out to be unstable as well. This means that with increasing time, no steady state is reached. The running away motion accelerates with time and the energy in the motion increases boundlessly. Figure 3.3 shows the surge, sway and yaw motions when not subject to an excitation, with a constant initial velocity of 1[m/s] or 1[deg/s].

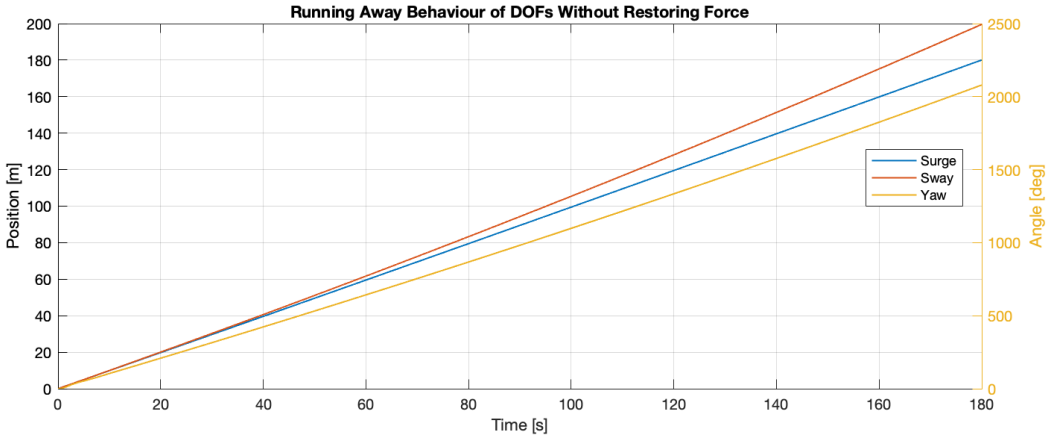

Figure 3.3: All degrees of freedom without a restoring force show running away behaviour. This graph shows how this motion can even accelerate with time. These predictions were made in the time domain.

When the retardation functions are looked at more closely, they appear to have a very small, or even negative, area underneath them. This poses a problem, since the damping is part of the retardation force. Sway's retardation function can be seen in figure 3.4. If retardation functions with a negative integral are to be convoluted with a constant past velocity, as was done to create figure 3.3, a negative damping is created, accelerating the ship, instead of slowing it down. This is however not only true for constant past velocities, also harmonic inputs will result in an average negative contribution by

the convolution integral. The integral of the retardation function of surge, way and yaw are all small compared to typical values in their respective damping curves. Typically, the value of the retardation integral is about a thousand times smaller than the average value of the damping curve, implying very little damping.

The exact value of the retardation integral is dependent on the maximum value of τ, since the retardation function shows small oscillations around zero, also for higher values of τ. For degrees of freedom with a very small area under the retardation function, these fluctuations have a relatively large impact on the ultimate value of this integral. Computing the retardation functions for larger values of τ seems to be an obvious path to diminish the effect of the tail oscillations. However, the frequency resolution, $\Delta\omega$, at which the damping coefficients are known, determines to what τ the retardation function can be resolved accurately. An absolute maximum τ is presented by $2\pi/\Delta\omega$, as the retardation function will be periodic with this period. The coefficients for the Acta Auriga are computed with a $\Delta\omega$ of 0.025 [rad/s], leading to an absolute maximum τ of about 251 seconds. Long before this time however, the retardation function has become jagged. This non-smoothness arises from the fact that for high values of τ, the damping curve is multiplied with a quickly oscillating cosine to determine the retardation function, see 2.15. When $\Delta\omega$, the frequency difference between two adjacent damping coefficients, becomes large, compared to the period of this cosine, the retardation function becomes rough. Practically, a $\Delta\omega$ of 0.025 [rad/s] allows for a smooth retardation function up to about 30 sec, which was used as τ_{max} throughout this project.

Whatever the exact value of the area under retardation functions for these degrees of freedom may be, it is very small compared to the damping curves. This leads to nonphysical results. In the frequency domain, any non-zero amount of damping will result in a bounded response to a harmonic excitation; it is a finite summation of sinusoids with finite amplitude. In the time domain however, running a simulation with coefficients based on the same damping may thus very well result in an unstable situation. This could, at least partially, originate from the frequency resolution at which the coefficients are known.

Adding frequency independent damping can be done straightforwardly to the hydrodynamic database when its intended purpose is to perform frequency domain simulations only. However, using this adapted data for time domain modelling turned out to require some care. Raising the whole damping curve by adding frequency independent damping means that the decaying tail of the curve is not converging to zero, but to the added frequency independent damping instead. Often however, also without adding damping, the high frequency tail will not be close to zero yet for ω_{max}.Therefore an exponential tail was fitted and appended, as described in section 2.5.1. When raising the damping curve however, the fitted tail might not yet have converged closely to zero either. This will affect the retardation function; persisting oscillations can in such cases be seen in the retardation function, affecting the predicted motions. This effect can be mitigated by fitting a longer tail, i.e. fitting to a higher maximum frequency. In the figure 3.4, three retardation functions are shown, one originating from the original damping curve, one from a raised damping curve, with the original fitted tail and one from a raised damping curve, with an extended fitted tail.

Adding damping greatly improves the match between the time and frequency domain results and mitigates the running away behaviour. Raising the whole damping curve by adding frequency independent damping, will mainly affect the low τ region of the retardation function, as can be seen in figure 3.4. This can be understood by considering Eq. 2.15; for low values of τ, the damping curve will be multiplied with a slowly oscillating cosine, before being integrated. For $\tau = 0$, the damping curve is multiplied with $\cos(0 \cdot \omega) = 1$, implying that $\kappa(\tau = 0)$ is directly proportional to the surface under the damping curve. For higher values of τ, the damping curve is multiplied with a cosine with more oscillations. When negative parts of the cosine are involved as well, the value of the retardation function for the τ under consideration will depend less on the absolute height of the damping curve, but more on the distribution of the damping over the frequencies. This distribution has remained unchanged by adding frequency independent damping. Therefore, for higher values of τ, the retardation function should look more similar to the original retardation function.

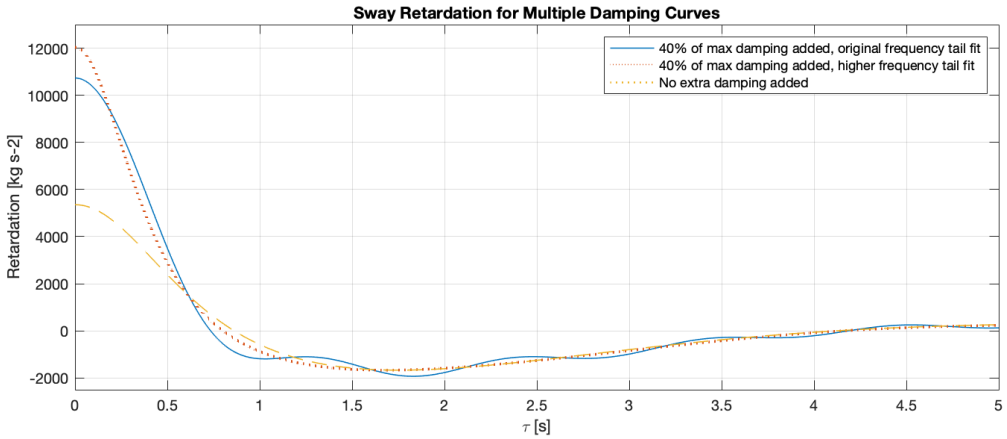

Figure 3.4: Sway retardation functions with different amounts of frequency independent damping and varying fitted high frequency tails.

Adding extra damping in the way described in the previous sections does not only change the results of the time domain simulations, but also those of the frequency domain. In case the frequency domain model is well capable of predicting the surge, sway and yaw motions, adding extra damping is unwanted; it decreases the response to a given excitation and will thus decrease the prediction quality. Surge is affected relatively little by adding damping; adding 100% of the maximum damping as frequency independent damping, results in a decrease of motion amplitude of around 1%. For sway and yaw this is around 26% and 20% respectively. Especially in sway and yaw, where damping is a relatively larger force in the equation of motion than for surge, changing the damping will seriously affect the motion amplitudes. This means that time domain modelling of sway and yaw needs a careful assessment of the desired extra damping. Adding more will result in a better match between the frequency domain and in less run away behaviour, but will decrease the motion response, wrongly, for a given input. In this project, the damping was added to better understand how the damping translates from the frequency to the time domain. Making the timestep smaller, also creates less runaway, no timestep size was however found that diminished the runaway behaviour altogether. In practise, using time domain modelling for surge, sway and yaw, there should thus be a balance between timestep and added damping.

To conclude, it is important to note that extreme runaway behaviour could affect the feasibility of time domain usage in real time seakeeping modelling, since coupling terms introduce an influence of surge, sway and yaw on heave, roll and pitch. These effects are included in the coupled equations of motion results, presented further down.

Roll Free Decay Instability

In figure 3.2, the roll time domain simulation performs similar to the heave and pitch prediction. This being true, a free decay test shows that the roll motion does not perform as expected. When a free decay test was simulated, the roll motion was not stable. A free decay test means that the vessel is brought to a non-zero steady state and is held stationary for a period, at least as long as needed to exclude the role of past velocities in the damping, before it is released. Heave, roll and pitch will all perform an oscillating motion during a free decay test with a real ship. Note that due to the absence of a restoring coefficient, it is insensible to speak of a free decay test for the other degrees of freedom. When looking at the free decay simulations, the comparison between the time and frequency domain is no longer normative, as the frequency domain is not capable of performing free decay simulations; only (a sum of) steady state solutions can be obtained. Figure 3.5 shows a free decay time trace of heave, roll and pitch.

For heave and pitch, a decreasing motion amplitude can clearly be seen. Roll however, does not decay and is in fact not stable; the amplitude of the motion increases with each oscillation, albeit ever so slightly. In contrast with surge, sway and yaw, the area under the retardation function of roll is positive. Enough damping is therefore available to stop a constant velocity motion. Besides the amount of

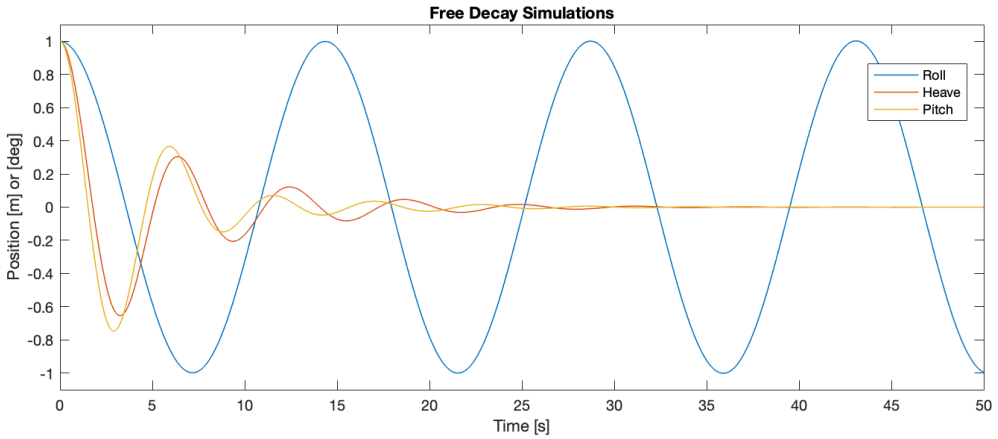

Figure 3.5: Free decay motions of heave, roll and pitch.Heave and pitch both show a nicely decaying curve. The roll motion however does not decay with time.

damping, the distribution over the retardation time τ is also of importance. For an arbitrary motion, this implies that the retardation force is not exactly out of phase with velocity as is the case for damping of a normal damped mass spring system. In the frequency domain, each frequency has it's own added mass and damping coefficient. In the time domain however, the infinte frequency added mass, A_∞, is only a single coefficient. To obtain the same result for a given frequency, the retardation function thus must distribute the force it creates; partly in phase with the velocity, the pure damping, and partly in phase with acceleration, the added inertia. How this distribution at a given frequency takes place is determined by the shape of the retardation.

In order for the retardation force to, at least partially, effect the motion like a damping force, it was assumed that the retardation force is to be more then $\pi/2$ [rad] out of phase with velocity. When this is the case, a component of the retardation function is π [rad] out of phase with the velocity, acting like pure damping, the remaining part will then be the added inertia. When the phase between the retardation and the velocity is smaller then $\pi/2$ [rad], the retardation force is partially in phase with the velocity, which was assumed to act as a negative damping. It was therefore hypothesised that motions at frequencies where the phase between the retardation force and the velocity was smaller then $\pi/2$ [rad], were not stable. At roll's natural frequency, the phase between the force created by the roll retardation function and the velocity is around $\pi/2$ [rad]. This means that almost all retardation force is in phase with the acceleration, acting as inertia force, and very little remains as damping, bringing the roll motion close to the edge of stability. The above described hypothesis does not explain the observed behaviour well; only at the natural frequency the roll motion was unstable. Motions at higher frequencies, where the phase was smaller, were in fact stable. The exact source of the instability is therefore not explained by looking at the phase difference between retardation force and velocity. An absence of damping does mean that no motion amplitude decay occurs, but does not explain an increase in motion amplitude, as was observed at the roll free decay test. The phase between the retardation force and the velocity is show in figure 3.6.

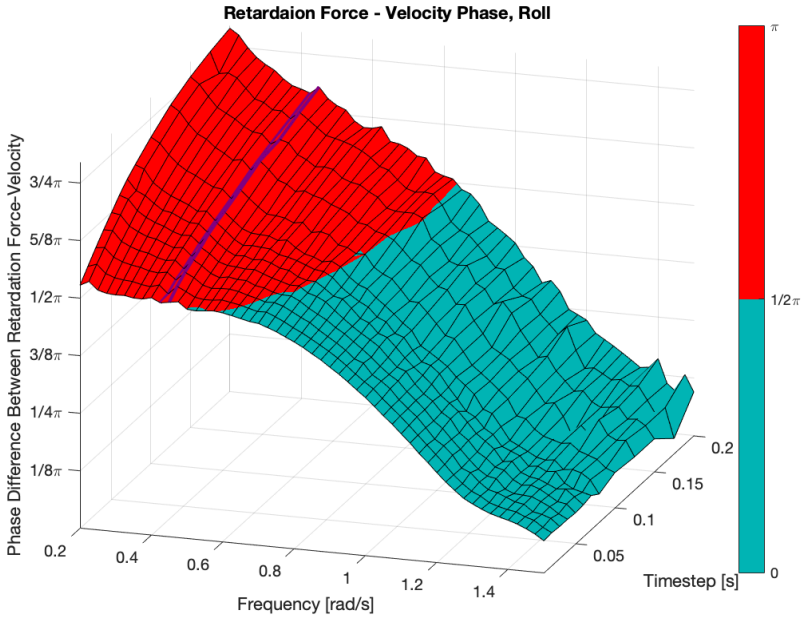

Figure 3.6: The phase between the force created by the retardation function and the velocity, for roll. The natural frequency lays between the two purple lines.

To conclude this section on roll instability, the energy in the free decaying roll motion is graphed in figure 3.7. Two means of determining the energy in the system were compared. Firstly, the total energy as the sum of the kinetic energy, $E_{\text{kinetic}} = 1/2mv^2$ and the potential energy, $E_{\text{potential}} = 1/2Cx^2$, was depicted by the solid blue line in figure 3.7. Secondly, the power delivered by the inertia, retardation and restoring forces, integrated over time, depicted by the red dashed line. Both describe the same behaviour, showing that all energy in the system indeed originated from these forces and not from some overlooked error in the code. The power of the inertial and restoring forces did not deliver net work, but did add fluctuations to the energy in the system. In accordance with the unstable free decay test, the energy in the system increased. It is worth mentioning that when the retardation force was not taking into account in a free decay test, the energy is exactly constant in time, as could be expected. This thus implies that the instability originates from the retardation force. The exact origins of this instability were not found. When roll damping was added, the roll motion became stable and the free decay test showed decaying amplitudes as well.

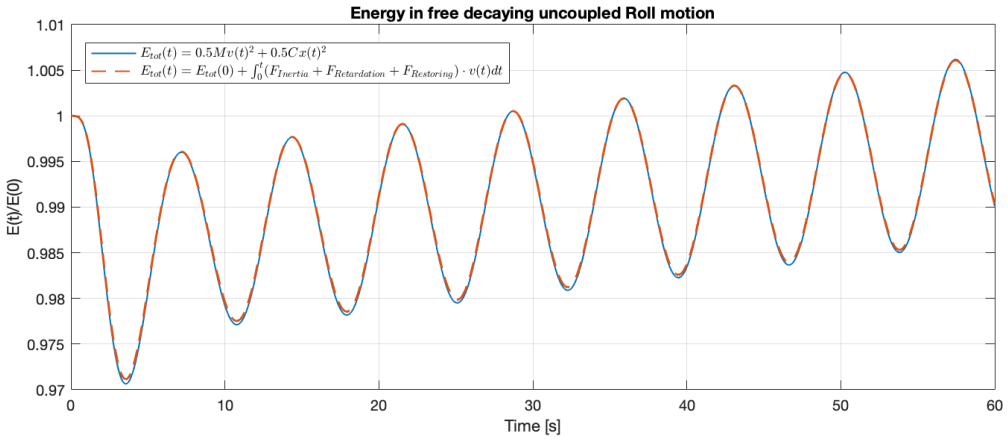

Figure 3.7: The total energy in the free decaying roll motion; it increases with time.

Steady State Error

The response to the Cummins equation was run for a large number of wave directions and frequencies. The difference between these outcomes and the results produced by the frequency domain equations of motion are calculated and referred to as the error. In figure 3.8, the amplitude error is given as a percentage. This is the difference between the time and frequency domain result, relative to the frequency domain solution. The phase errors are shown in appendix A.

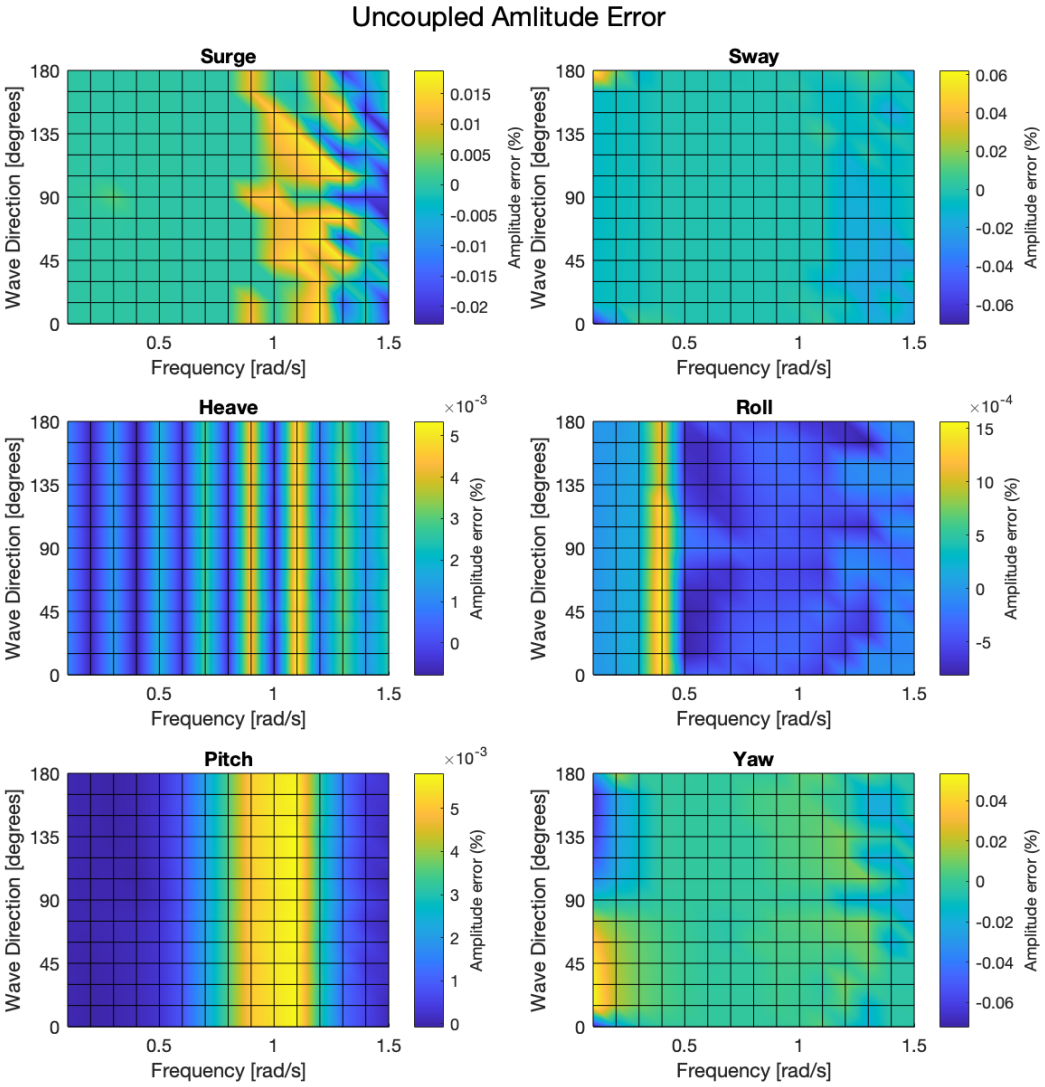

Figure 3.8: The difference between the time and frequency domain motion amplitudes. Positive values indicate that the time domain amplitudes were higher than the frequency domain amplitudes. The running away behaviour of surge, sway and yaw was corrected for to obtain sensible values for the amplitude error.

3.1.2. Uncoupled Motions, Spectrum Excitation

The next step in complexity is to not excite the system with monochromatic forcing, but with a spectrum instead. This spectrum consists of multiple frequencies, the different components have different force amplitudes and phases. In reality, the spectrum may have various forms. A fully developed sea state is however well described by the JONSWAP spectrum [9]. Figure 3.9 shows the uncoupled responses to a JONSWAP spectrum excitation, with a wave direction of 65 degrees, as this angle excites all degrees

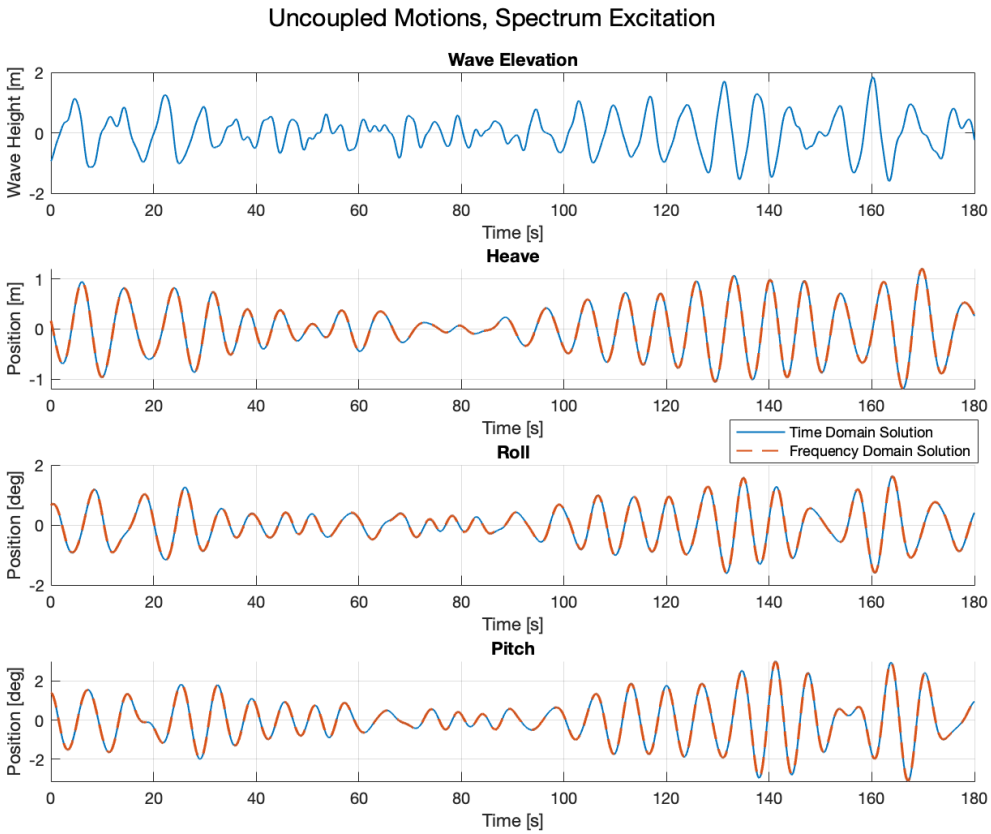

Figure 3.9: Uncoupled degrees of freedom, spectrum excitation response.

of freedom nicely. The spectrum used here corresponds to a fully developed sea state at a windforce of 5 Beaufort.

Time and frequency domain models seem to correspond well in figure 3.9. Further investigations showed that this good match is not guaranteed for every condition. The spectrum shown here contains 160 different frequencies. These frequencies are the same as the ones in the hydrodynamic database. The total response thus contains only frequencies where the RAO is known for; no interpolation takes place. If this condition is not met and frequencies at positions other than those were the RAO is known for are present in the spectrum, the match between time and frequency domain is lost. The severity of the difference between time and frequency domain results depends on the windforce, and thereby on the power distribution over the frequencies in the spectrum. When the wind becomes stronger, the peak of the spectrum shifts to lower frequencies [[9]]. This means that relatively more energy will be present in frequencies close to the resonance peak for roll. This is only a problem when interpolation is to take place between frequencies. Interpolation along the frequency axis is either needed when the frequencies of the spectrum are not chosen according to the data in the hydrodynamical database or when the frequency step in the excitation spectrum is smaller than in the database, in which case there is no possibility to match the excitation and hydrodynamical database frequencies. The consequences of this are shown in figure 3.10. This phenomenon is only present for the roll motion and it seems to originate from the interpolation in the RAO.

Interpolation in the Roll RAO

The effect of interpolation in the frequency domain on the results in the time domain originates from the fact that a velocity history in the time domain is applied, this was done to start the simulation with a physical amount of damping and was described on page 18. This is needed to obtain stable time

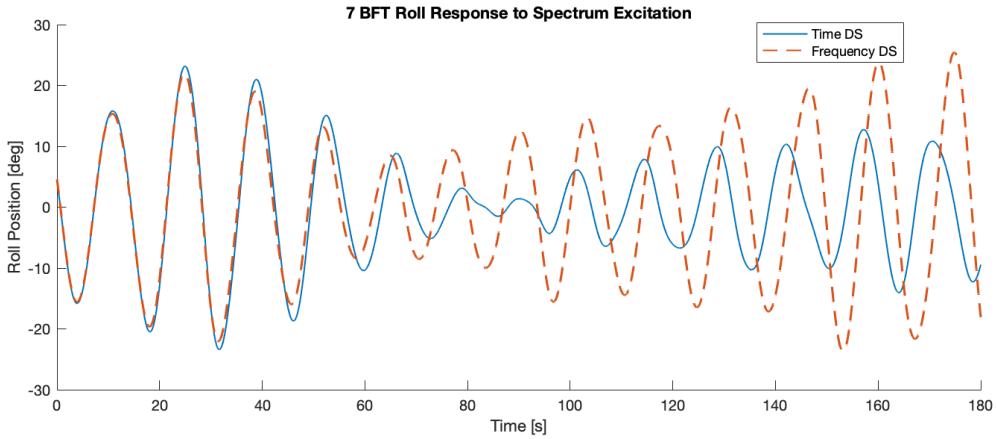

Figure 3.10: More severe sea states make the roll response to a spectrum excitation deviate from frequency domain results.

domain solutions for roll. These past velocities are obtained from results in the frequency domain, since no time domain results are available for $t < 0$.

A system at, or close by, resonance is dominated by its damping. When the damping force is small compared to the inertia and restoring forces, as with the roll motion, a small change in damping will make for a large change in the response amplitude. When using a historic velocity obtained by interpolation in the frequency domain to pre-load the damping, errors in the interpolation are relevant. Moreso, because of this small damping, the roll RAO will be much more peaked compared to more severely damped systems, i.e. heave or pitch. This makes for larger interpolation errors. Roll motions are thus more susceptible for RAO interpolation errors, and the interpolation errors are larger, compared to other degrees of freedom.

When the provided historic velocities are either too high or low, the resulting damping will not match the steady state motion. For a lightly damped degree of freedom as roll, this will result in an extra wave pattern in the motions. When the historic velocities are lower than the steady state velocities, there will be too little damping, resulting in an increase in motion amplitude. This increase will however overshoot the steady state motion, due to the low damping, resulting in too large amplitudes. This in turn will result in damping higher than needed for the steady state, leading to a decrease in amplitude which will again overshoot; a wave pattern on top of the normal steady state motion. This means that wrongly sized velocity histories, originating from interpolation errors in the RAO's, lead to considerable errors in the time domain roll motions.

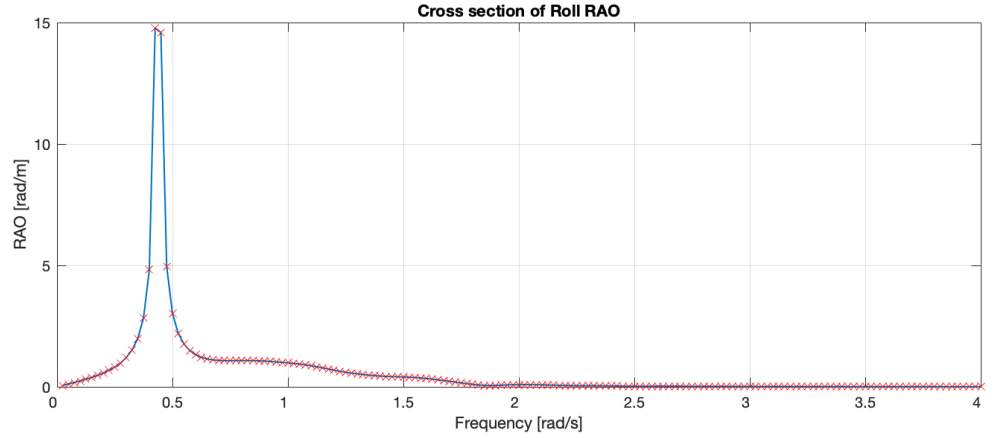

Figure 3.11: A cross section off the Roll RAO, note the extreme peak at the resonance frequency.

Around, and mainly at the resonance frequency, the RAO is strongly bent, see figure 3.11. Performing linear interpolation is clear to 'cut corners' and will thereby introduce a considerable error. No other degree of freedom's RAO shows curvatures comparable to that of the roll RAO. Using different interpolation schemes helps mitigate the above described waving pattern, however, it is never completely removed. This means that producing sensible spectrum responses for more severe wave states is still not possible when having frequencies in the excitation that differ from the frequencies in the hydrodynamical database.

In an effort to eliminate the errors introduced by interpolation, the RAO was supplemented with values at extra frequencies. This was done to see if more trustworthy spectra responses could be obtained, which are needed for Next Ocean's functionality. When the time domain results are deemed trustworthy for frequencies where a correct historic velocity is known for, the time domain solution can be used to create extra values in the RAO. This is done by tuning the amplitude of the past velocity until no amplitude waves are present in the time domain solution. The motion amplitude corresponding to the past velocity for which this is true is then taken as the RAO value for the corresponding frequency. This procedure is time consuming, as for each amplitude change of the past velocities, the time domain code is to be ran again and this is to be done for a large numer of frequencies and directions. The procedure works well for the region around the resonance peak, right at the peak however, the alterations that are to be made are much more severe and should also include changing the phase of the past velocity. Finding the exact RAO value there was more difficult than deemed sensible for this project, therefore this way of making the spectrum responses of roll more reliable was abandoned. Figure 3.12 shows a zoomed in section of the curved roll RAO, with multiple interpolation schemes, as well as the reconstructed RAO values.

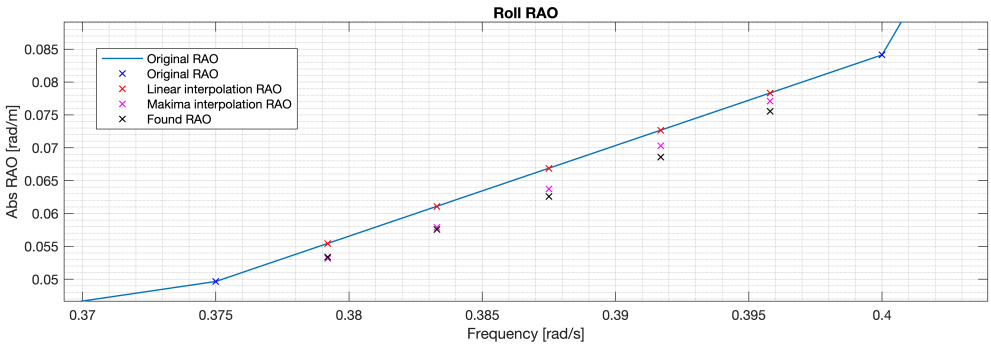

Figure 3.12: Different interpolation schemes, along with the reconstructed RAO, show how linear interpolations introduces errors in the motion amplitude of the past velocities provided to initialise the roll calculation.

A second important thing regarding the interpolation for frequencies between the top two values, i.e. $0.425\,[\text{rad/s}] < \omega < 0.45\,[\text{rad/s}]$, is that the phase phase turns approximately 180 degrees. This happens in one $\Delta\omega$. When interpolating the phase and amplitude as two separate numbers, the phase will come out wrong; it will decrease from its maximum value, via zero, to its minimum value. When interpolating in the complex plain, the phase change will occur more abruptly, as is physical. Interpolating in the complex plane will however not produce correct RAO amplitudes; this too will then go from a very high value, via zero, to a very high value again. While in reality it reaches a maximum somewhere between these frequencies. The amplitudes should therefore not be interpolated in the complex plane. The above described phenomenon can be visualised in figure 3.13.

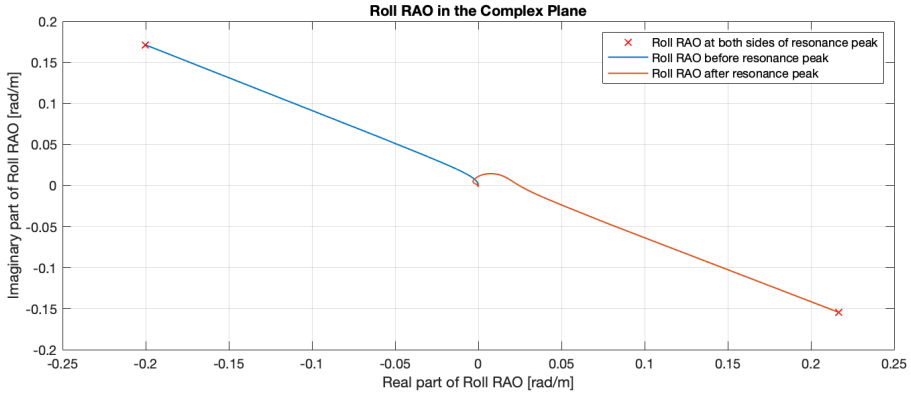

Figure 3.13: The roll RAO in the complex plane. Note the extreme absolute value of the roll RAO; the red crosses are the only points at the extreme distance from the origin. Other DOF's show a much more curved, less extreme RAO.

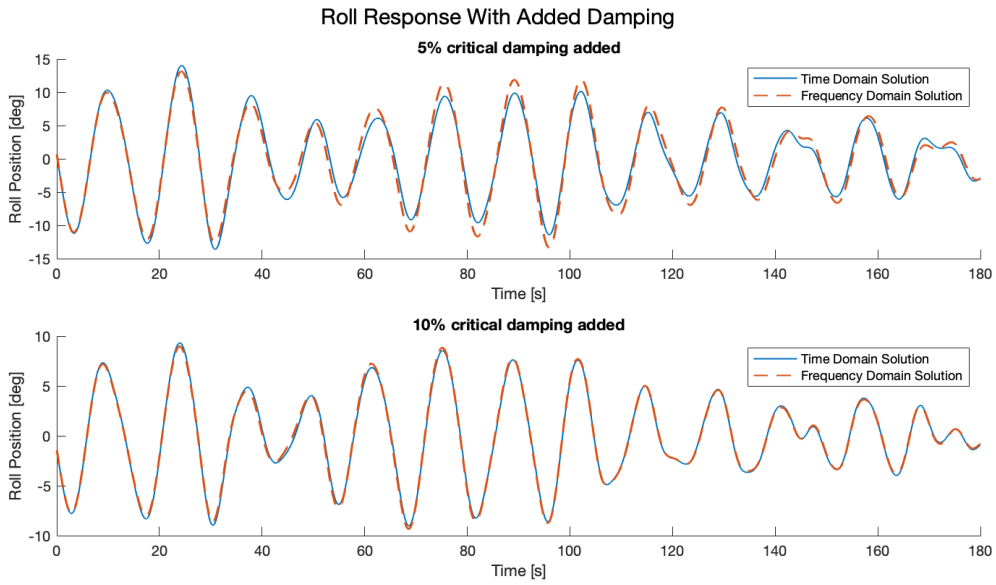

Figure 3.14: The added damping closes the gap between time and frequency domain results. Note the changing motion amplitude by adding damping.

As was done for surge,sway and yaw, extra damping was added to see if this behaviour that was attributed to a lack of damping, was indeed gone when damping was added. Figure 3.14 shows the responses to an identical excitation spectrum, for different amounts of added damping. This 7 BFT spectrum consists of much more frequencies than the hydrodynamical database contains. This clearly shows that adding damping indeed makes the time and frequency domain results look much more alike. Note here as well, the motion amplitude itself is highly effected by adding dampin.

3.1.3. Coupled Motions, Single Frequency Excitation

After the uncoupled motions were looked at into detail, the coupling between degrees of freedom was introduced. In real vessel motions, the coupling is always present, therefore this coupling will also need to be used when re-predicting the motions with the newly identified parameters. The following sections show results that were produced with the coupling being present.

Poor Tail Fitting

Coupling the degrees of freedom to each other entails that more retardation functions come into play. The equations of motion will become a coupled system of equations, where each equation contains three different retardation functions. One of them is concerned with the damping from the motion it-

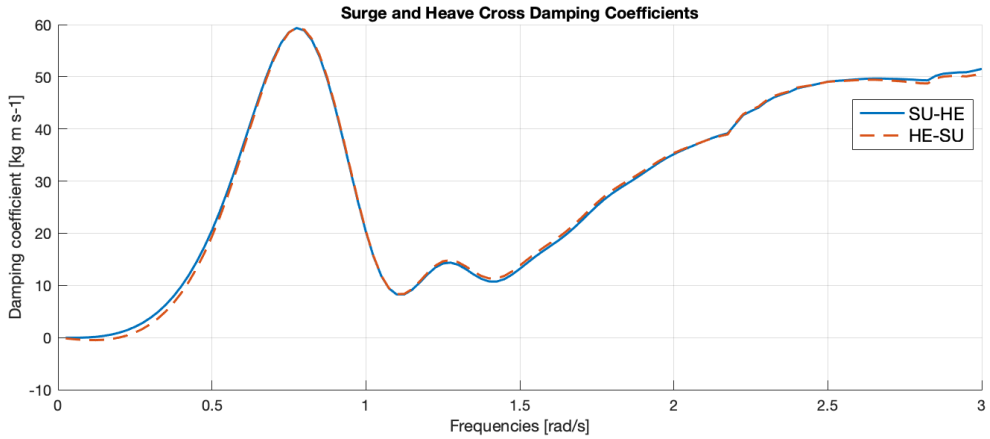

Figure 3.15: The dampingcurve for the crossterm between surge and heave.

self, and was also used in the uncoupled equations described earlier. The other retardation functions originate from the off diagonal damping terms. Most of the off diagonal coefficients show a comparable curve as the on diagonal damping coefficients. The coupling between surge and heave however, results in a highly different damping curve, as can be seen in figure 3.15. No sensible tail fitting can be performed for these curves.

Retardation functions based on these damping curves shows much more oscillations, since no tail can reasonably be fitted to this damping curve, as can be seen in figure 3.16. These oscilations for high τ values were also observed when damping was added, without adding longer fitted tails, see page 21.

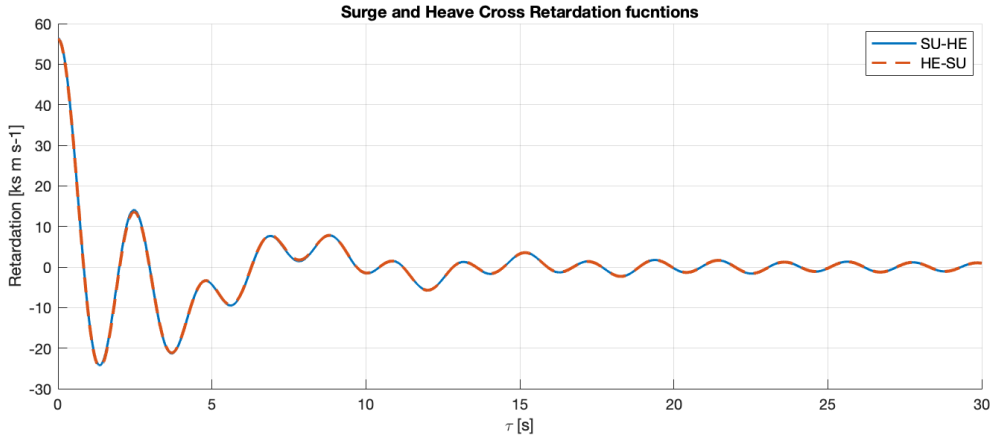

Figure 3.16: From the damping shown in figure 3.15, these retardation function were obtained. Note that the oscillations persist for high τ values.

The resulting infinite frequency added mass coefficients also shows deviating behaviour, see figure 3.17.

This particular coupling term is not of great importance, as the forces and moments involved are small compared to other forces for both heave and surge. For different vessels, this is not necessarily the same; different hull forms may change the relative importance of coupling terms. In general, finding the hydrodynamic coefficients for high frequencies may therefore be of even more importance for other vessels. Although it cannot be concluded from figures 3.15, 3.16 and 3.17 that the panelling of the hull is responsible for the remarkable damping curves, the graphs go to show that much attention should be paid to the panelling when determining the hydrodynamic coefficients as data for higher frequencies is needed to be able to fit a sloping tail to the damping curves. Damping curves, retardation functions and added mass curves for all coupling forces are shown in appendix B.

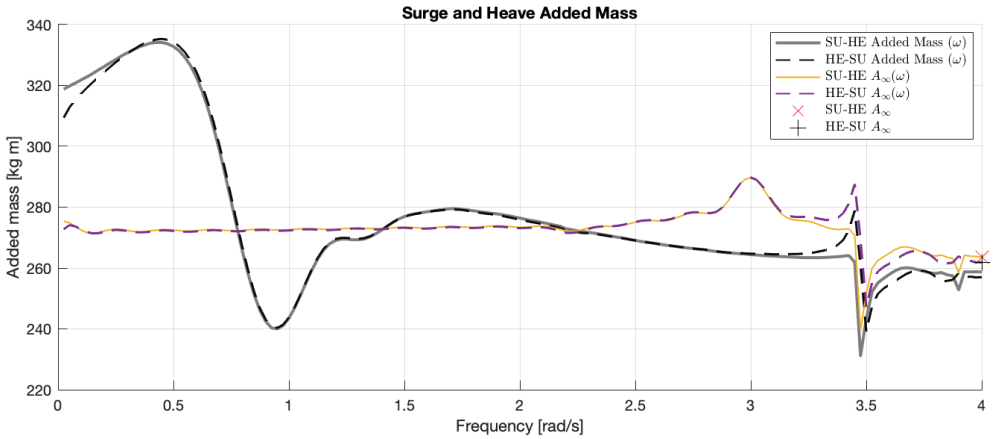

Figure 3.17: From the retardations shown in figure 3.16, these added mass curves were obtained; It is much less clear what value to choose for A_∞.

Steady State Errors

Also the coupled Cummins code performance was tested against coupled frequency domain results. In figure 3.18 the running away behaviour of surge, sway and yaw was corrected for to obtain sensible values for the amplitude error. The amplitude of these degrees of freedom is thus determined after detrending of the surge, sway and yaw results.

The errors in the phase are shown in appendix A. Compared to the uncoupled case, shown in figure 3.8, a more clear wave direction dependency can be seen. The larger errors can mainly be seen at wave directions where the response of that degree of freedom is very low. At those wave directions, the coupling forces are of relative high importance. The error could occur from an error in the coupled degree of freedom and as both sets of coupled motions contain at least one non restoring degree of freedom, the effect of the running away behaviour might be visible here. Another possibility is that these large errors arise simply from the fact that the response is very low, meaning that the small absolute errors lead to large relative errors.

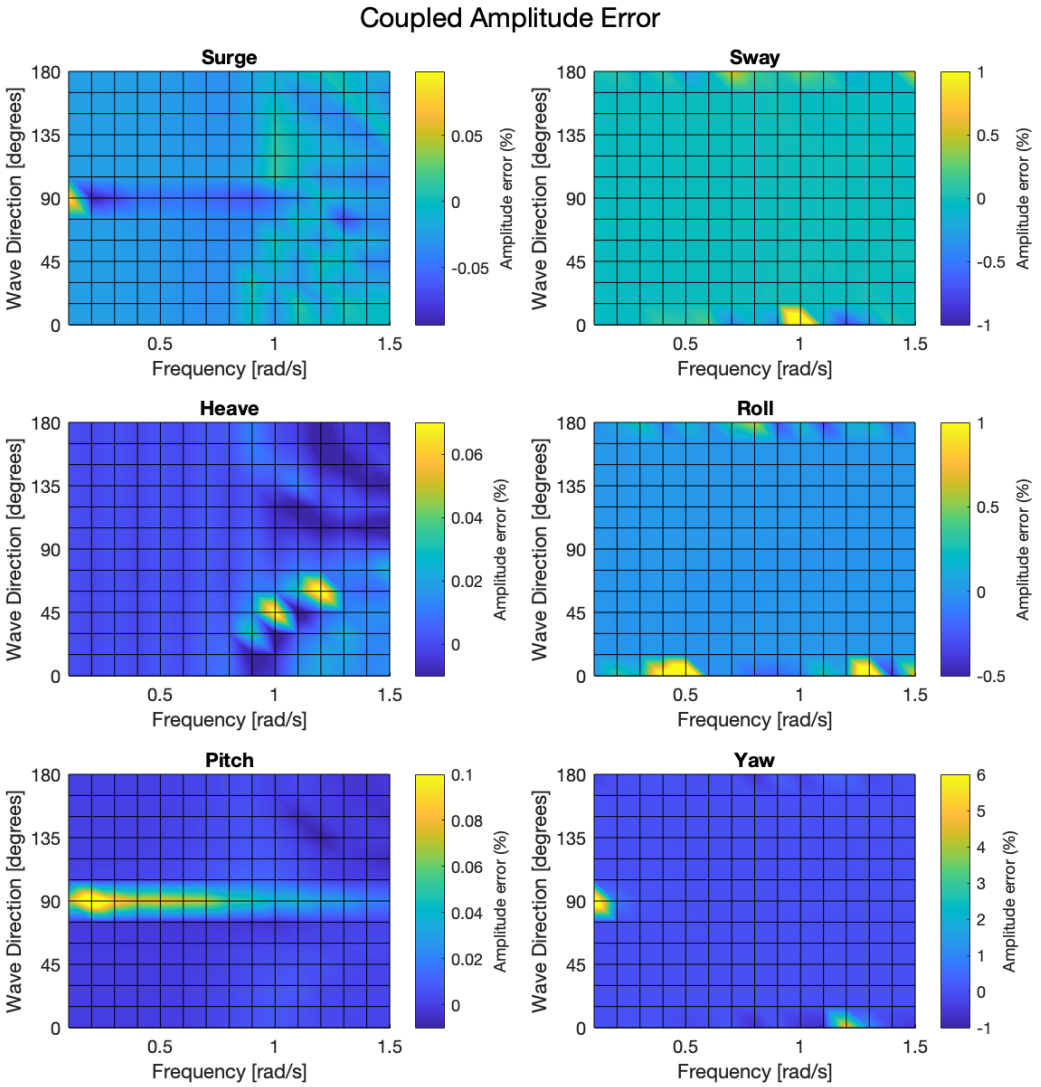

Figure 3.18: The steady state difference between frequency and time domain amplitudes of coupled motions. The error is determined as a percentage with respect to the frequency domain results, as was done for figure 3.8.

3.1.4. Coupled Motions, Spectrum Excitation

The final and most realistic simulation is coupled and takes a spectrum excitation as input. Figure 3.19 shows responses of heave, roll and pitch to a spectrum excitation.

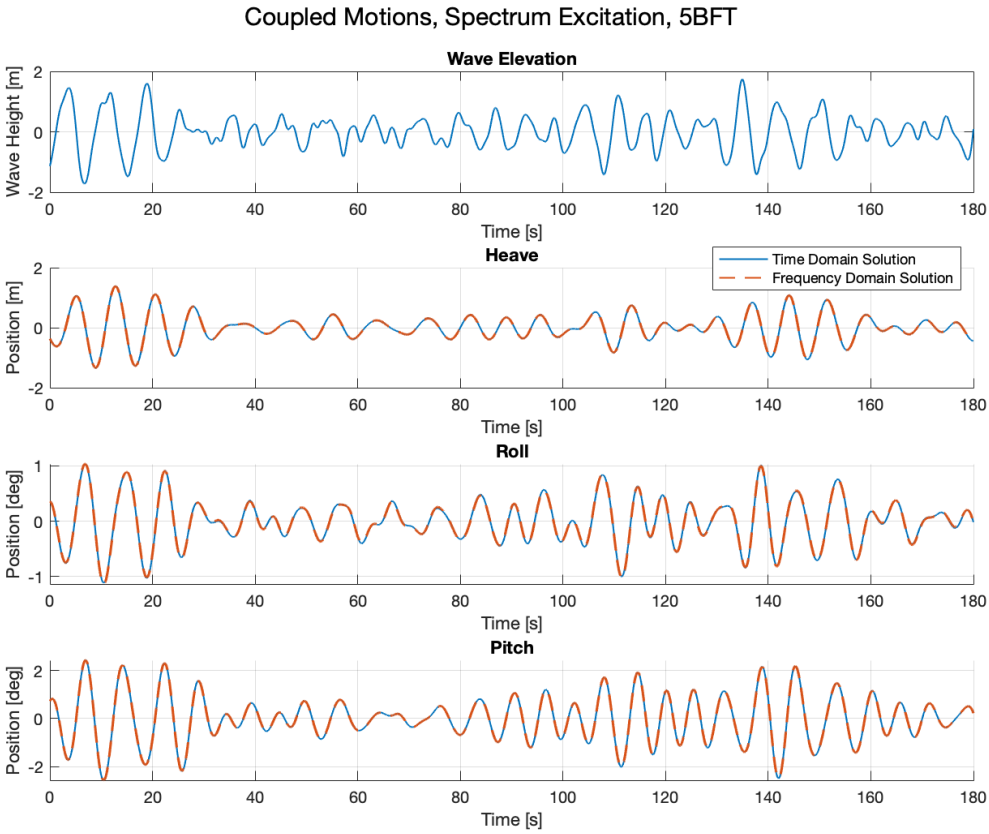

Figure 3.19: Coupled degrees of freedom exposed to a spectrum excitation are the most realistic type of synthetic experiments.

For the coupled spectra excitation, the same holds as for the uncoupled counterpart; damping should be added to be able to model more severe seastates with many frequency components. The match between time and frequency domain models was deemed sufficiently good to proceed with parameter identification.

3.2. Parameter Identification and Re-Prediction

The second part of the results section elaborates on the performance of the time domain code, with the use of newly identified parameters. First, the steps taken to make the field data ready for re-prediction are described, followed by the results of the re-prediction itself.

3.2.1. Field Data Processing

In the re-predictions, the predicted excitation forces, produced by the Next Ocean system onboard the Acta Auriga are used. The data was gathered on the 4th and 5th of may, 2021. The vessel was operating in the North Sea at that time. The sea state was light to moderate; the significant wave height was in accordance with a windforce between 4 and 5 BFT. All identifications and re-predictions in this project were performed with these hours of data.

The data produced by the Next Ocean system is wrongly scaled. This has its origin in the way a wave radar works; the received energy is assumed to be proportional to the steepness of the waves, among other things. The shape of the wave field can be determined from this information. This wavefield will

however be wrongly scaled, meaning that the resulting excitations do not have the right amplitude. In order to work with these excitations, they have to be scaled. Besides scaling, the raw data may be shifted too. This shifting and scaling is done by Next Ocean too. Next Ocean uses algorithms that change the shifting and scaling through time, to ensure an as good as possible fit for the predicted motions. The time varying character of the refined force data made further processing cumbersome. Therefore raw data was used, which was still to be scaled and shifted.

Multiple ways of going about the scaling and shifting were considered and tested. These varied in complexity. The algorithms differed in: (1) whether they used time varying scaling and shifting and (2) whether degrees of freedom would each get their own scaling and shifting or if one scaling and shifting was chosen for all degrees of freedom.

Time varying shifting and scaling is relevant in real applications, as the circumstances where the system operates may change rapidly. Therefore, the optimal scaling varies from time to time. The data used in this project however was recorded during a relatively constant sea state. Considering the optimal scaling for adjacent segments in time, see figure 3.20, shows that time dependent scaling seems to be not needed, as little variations in the optimal scaling were found. This made for the usage of a more robust and transparent non varying scaling algorithm. Regarding the choice of from what degree of freedom to take the scaling factor from; it was deemed more physical to choose one scaling for all degrees of freedom, as there is only one wave field surrounding the vessel. As is shown in figure 3.20, there is a considerable difference between the optimal scaling for each degree of freedom. The heave and pitch scaling coefficient are much alike. These degrees of freedom are also important to predict right as they are often a determining factor in deciding on proceeding or abandoning an operation. Also, when rightly pre-processed forces are used, these degrees of freedom are most likely to produce trustworthy results. Therefore, the heave scaling and shifting was chosen to be used for all degrees of freedom.

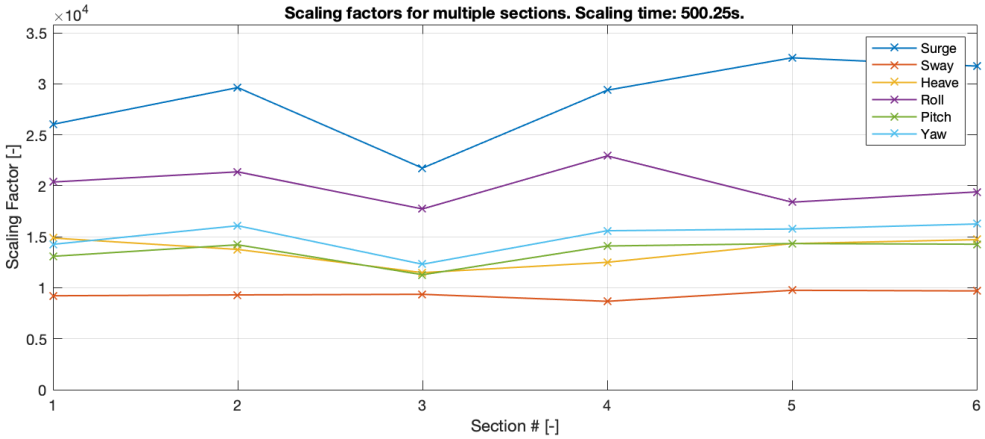

Figure 3.20: Scaling factor deviate only slightly through a section of time. Heave and pitch show similar scaling factors.

Field Data Segments

Multiple hours of field data was available to perform identifications and re-predictions. These hours were selected based on the quality of the heave, pitch and roll predictions. A relatively high quality for these predictions ensured that a certain minimum amount of correct information was present in the predicted excitation forces. This data came in segments with a length of approximately one hour. Typical Next Ocean predictions have a length of up to approximately 3 minutes. In order to reasonably assume that the scaling and shifting do not vary significantly throughout one segment, the blocks of an hour length were divided into smaller segments, of several minutes. As discussed above, in such a block one single scaling and shifting was used. For each such block, identification and re-prediction was performed.

Scaling the Excitation
The predicted excitation was scaled using the measured motions. Therefore, the unscaled predicted forces are translated to unscaled predicted motions. This is done using the RAO. Since the raw predicted forces are too large, motions with a too large amplitude are obtained. These motions are then compared to the measured motions in order to obtain a scaling factor. This is done using the root mean squared value of both signals. The scaling factor γ is determined from this as follows:

$$\gamma = \frac{\text{RMS(Predicted Motions)}}{\text{RMS(Measured Motions)}}$$

As shown in figure 3.20, the scaling factors are typically far away from unity, making the fact that the RAO is a linear function highly valuable. Also because of the linearity, the same scaling factor can be used for the unscaled excitation forces.

Shifting the Excitation
Besides scaling, the predicted forces are also shifted. The need for a shift originates from delays and the timing in the radar system. Also the ideal shifting may vary with time, but in this thesis, one shifting value is determined for one segment of time. The optimal shifting is determined using the cross correlation function. Again, the scaled predicted motions and the measured motions are used. The shift at which the maximum cross correlation occurred was deemed optimal. A maximum shift was set, as unrealistically large shifts could occasionally lead to higher correlation values. Figure 3.21 shows three different signals; the measured motion, the scaled but unshifted predicted motion and the scaled and shifted predicted motion. Again, the same scaling and shifting found for the motions, was applied to the predicted forces.

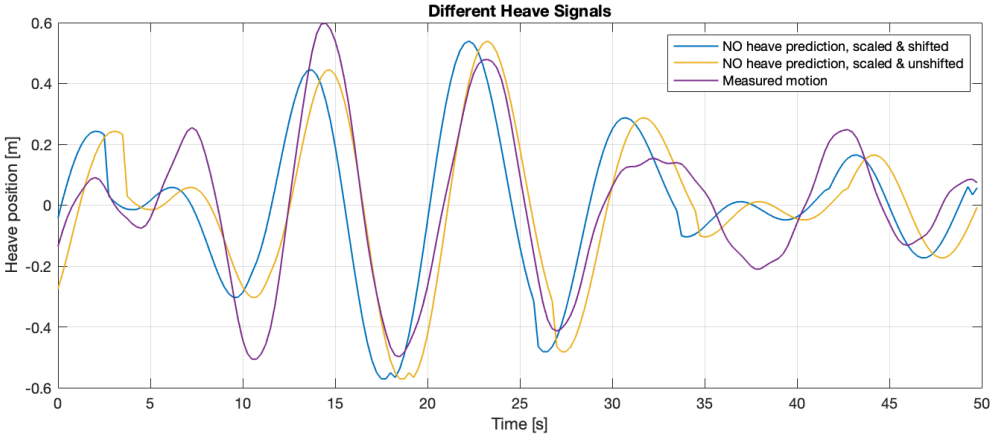

Figure 3.21: The shifting of the predicted signals ensures an as good as possible prediction.

3.2.2. Re-predicting, No Identification

As described earlier, differences between time and frequency domain results are present. It can therefore not be assumed that the Next Ocean predictions, made in the frequency domain, will match the time domain predictions, with similar input and coefficients, perfectly. Besides the errors described in earlier sections, also the provided historic velocities play a role in this. In the synthetic case comparisons between the different domains, the time domain was provided with past velocities from the frequency domain, setting it up for success. In real time usage of the time domain code, the past velocities would be taken from motion measurements. Since there can be a considerable difference between the Next Ocean prediction and the measured motions, the time domain re-predictions could differ severely from the Next Ocean predictions. Since roll showed an exceptional dependency on the past velocities provided, especially at frequencies around resonance, it is to be expected that the differences between time and frequency domain predictions for roll are larger than for other degrees of freedom. This is further enhanced by the fact that Next Ocean's roll predictions are often worse than the predictions for the other degrees of freedom. The quality of a prediction is expressed by the correlation between the

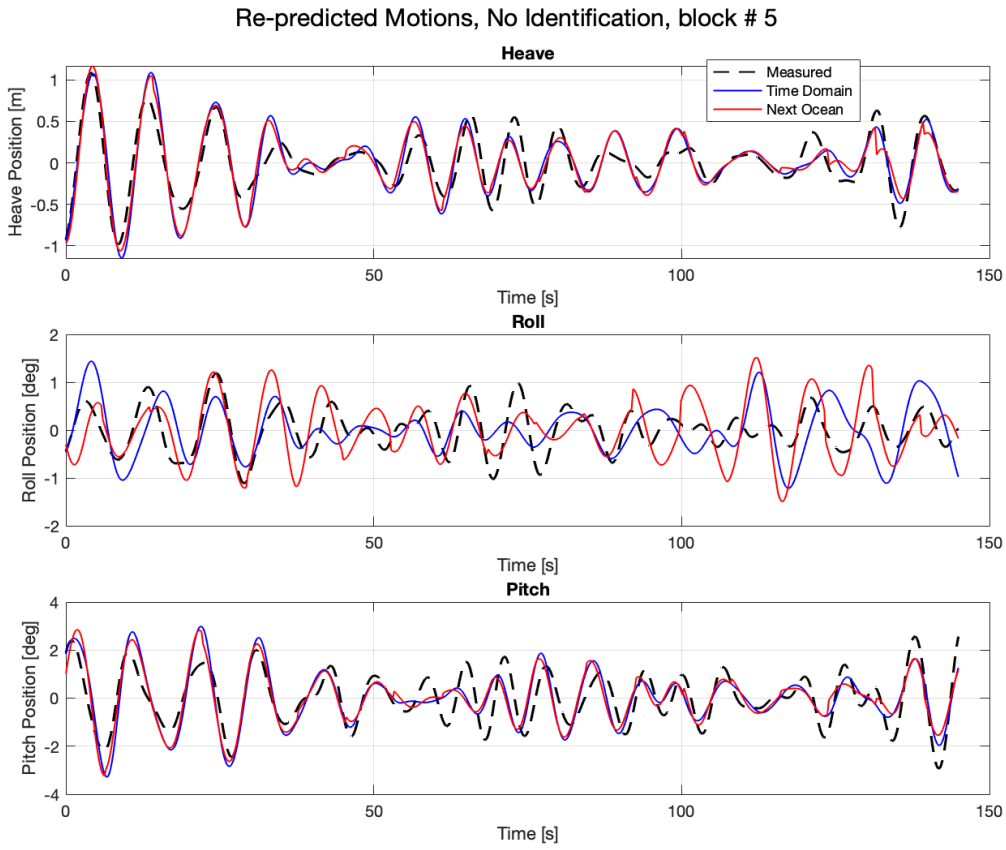

Figure 3.22: The time domain re-prediction, without updated or added coefficients.

prediction and the measurement. Graphs of correlation coefficients for predictions made with adapted function coefficients are shown in the following sections. To give an idea on how the different degrees of freedom time domain re-predictions perform, figure 3.22 is shown.

As expected, it can clearly be seen that the time domain roll re-prediction is of much lower quality than that of heave and pitch. The correlations between the Next Ocean predictions and motion measurements and the time domain re-predictions and the measured motions are shown in figure 3.23. Both heave and pitch show very similar correlations for each time segment. Time domain roll re-predictions however, show a much lower correlation with the measured motions. This is in accordance with what is depicted in figure 3.22. In order for this project to have a positive outcome, the correlations between re-predicted and measured motions should be higher than the correlation between the Next Ocean predictions and the measured motions.

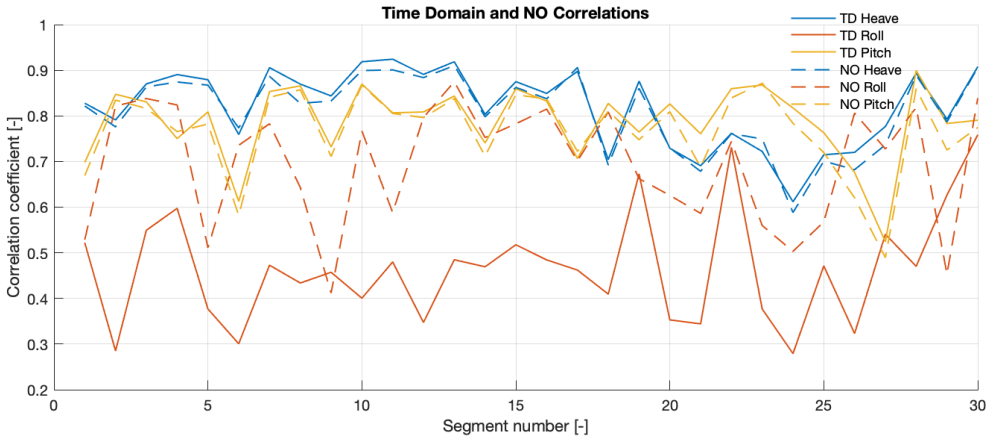

Figure 3.23: The correlations of the time domain re-predictions are considerably lower then those obtained by Next Ocean, especially for roll.

3.2.3. What Coefficients to Identify

The main aim of this project was to improve roll predictions, using adaptive damping coefficients. It is therefore natural to identify roll damping coefficients from the moment residuals. As described in section 2.4, it was intended to fit a third order polynomial through the residuals. The found coefficients will be presented shortly. Other force coefficients could be identified too, as described. In order to determine what forces may be eligible for this, the force and moment residuals were plotted against all relevant motions and its time derivatives. For roll, these motions include sway and yaw motions, besides roll itself. Coupling forces between these degrees of freedom may depend on the velocity, accelerations and sometimes positions of all three DOF's. The moment residuals for roll, see equation 2.21, are shown in figure 3.24.

Note that for each time segment of field measurements, plots as shown in figure 3.24 can be made and although the exact value of the correlation can vary, typical values can be observed. It is important to mention that the correlation value does not give information on how high the coefficient will be. A very strong correlation means that the points lay neatly on a line, but the steepness of that line is not captured in the correlation value. A strong correlation may therefore still mean that a low force coefficient will be identified, or vice versa.

The roll moment residuals are not strongly correlated with roll velocity. Sometimes, the correlation is negative, and for re-prediction with an identified roll coefficient this poses a problem that will be discussed later. There was also little correlation between $\dot{x}_{4,4} \cdot |\dot{x}_{4,4}|$ and the residuals and between $\dot{x}_{4,4}^3$ and the residuals. Since the initial idea of this project was to identify roll coefficients, identifications of these forces were still performed, despite showing low correlations. Residuals of other degrees of freedom are shown in appendix C.

Considering the roll residuals in figure 3.24, potential other forces to identify are the roll and yaw induced inertia forces, as well as the roll and yaw induced restoring forces. The last of these forces is however not present, as yaw position can never induce a restoring force, identifying this coefficient was therefore not done. For the other degrees of freedom, pitch velocity induced pitch moment is the only consistently high correlation. The results of these re-predictions are discussed in the following section.

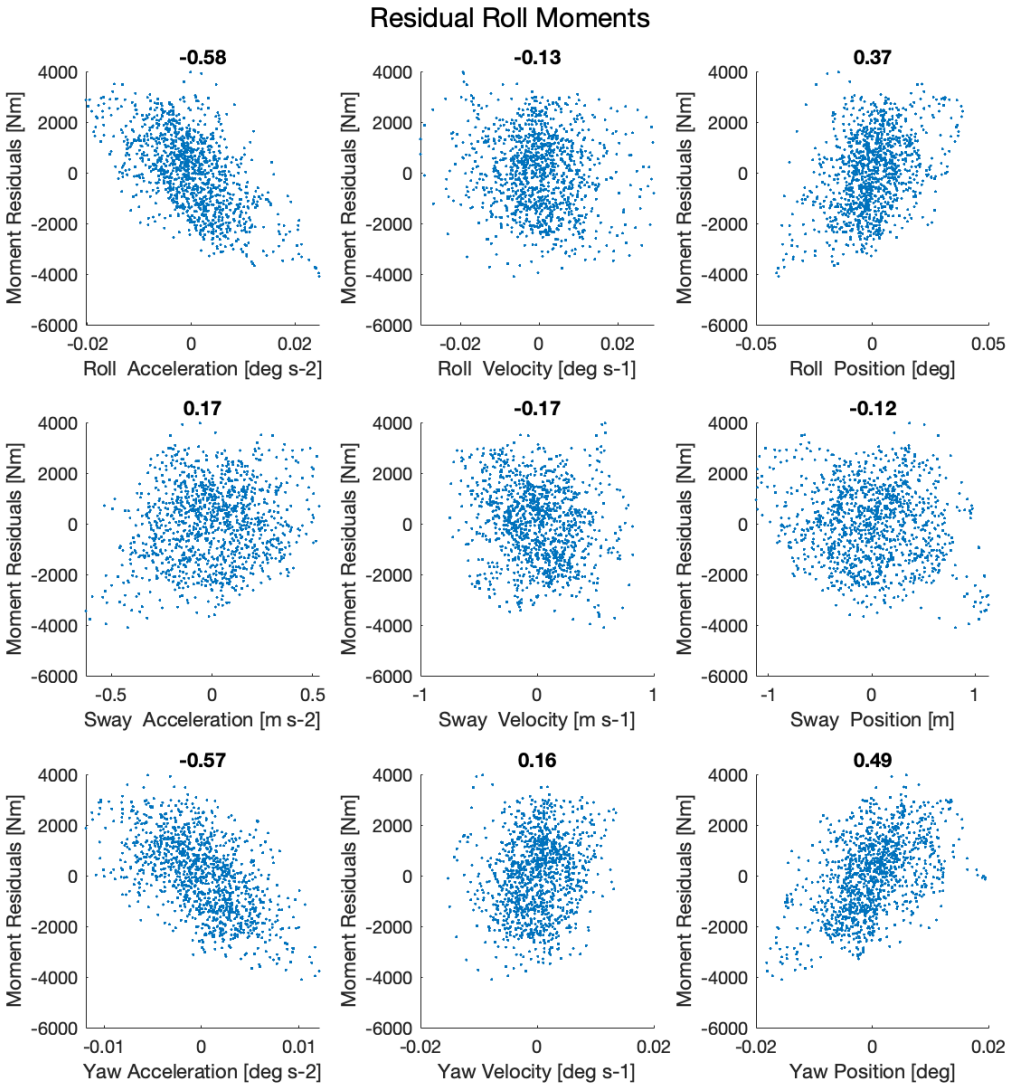

Figure 3.24: Roll moment residuals. Each dot represents a measurement. The title of each sub-graph is the correlation coefficient.

3.2.4. Re-predicting, With Identification

The previous section described that despite the low correlation between roll moment residuals and different powers of roll velocity, a fit for the roll damping coefficients was performed. Figure 3.25 shows the identified coefficients for added linear, quadratic and cubic roll damping forces.

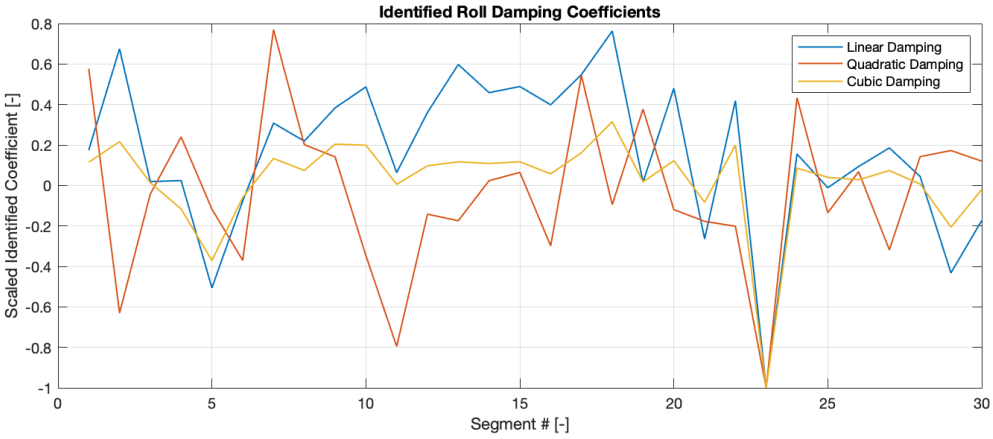

Figure 3.25: The identified roll damping coefficients show a wide variation.

Note that the coefficients are normalised to make them visible in a single plot. The highly varying character of all three curves, as well as the fact that all three curves show negative values for multiple segments is of prime importance. The highly varying value of the best fitting coefficient shows that no single value for each of the coefficients can be found. This is in accordance with the fact that a low correlation between the roll moments and the velocity were found. No roll damping coefficient could be found that seems to belong to the vessel; it varies largely from segment to segment, making that it can not be reasonably expected that an identified coefficient will be suitable to improve predictions in the next segment. Some identified damping coefficients are negative. This leads to unstable re-predictions, as the roll already had low damping to start with. Adding a negative damping lowers the damping further and makes the roll motions unstable. In cases where a positive coefficient was found, the correlation was in general not improved when compared to the performance of the Next Ocean predictions. This is shown in figure 3.26.

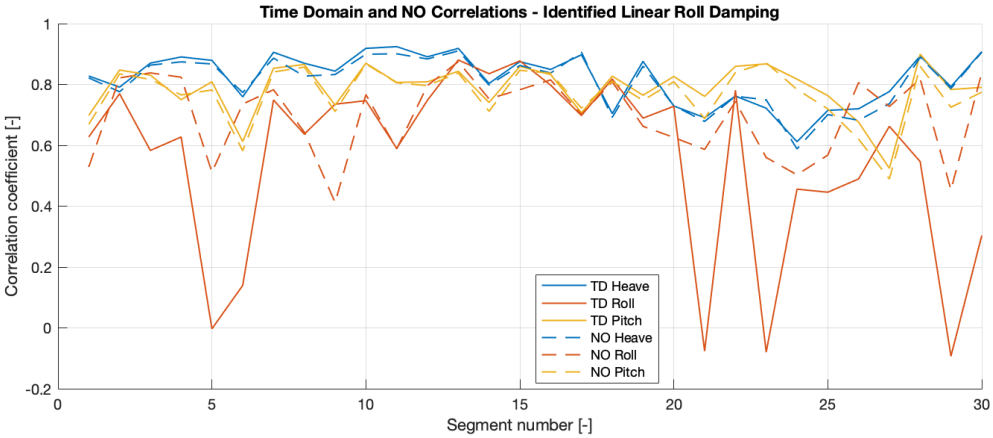

Figure 3.26: Correlation coefficients of the re-predicted roll motions, using identified linear roll damping.

Important to mention is the fact that the coefficients identified have now been used to re-predict the same section of time that the identification took place in. In real applications however, the identification has to be performed on earlier sections. This shows the importance of a more or less constant coefficient; otherwise it would be impossible to know what value fits the coming section. When the re-prediction is done using a coefficient that was identified in the previous segment, as would have to

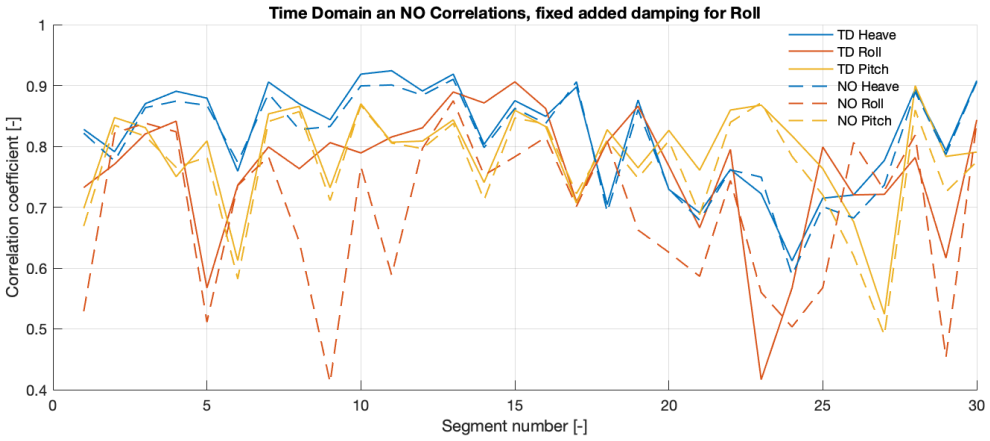

Figure 3.27: Adding a fixed amount of linear damping led to improved results, compared to predictions performed by Next Ocean.

be done in the real application, the correlations lower further.

Besides identifying a damping force coefficient, a fixed amount of linear roll damping was added to the equation of motion as well. This resulted in an improved performance for most segments. Correlation coefficients for these re-predictions are shown in figure 3.27. The slight performance enhancement of on average 9.57% reached by adding a fixed amount of damping might be beneficial in real applications. It is however not a result of identification, nor is a simulation in the time domain needed. Adding frequency independent damping can straight forwardly be done in the frequency domain, as was discussed in section 3.1.1.

The amount of added damping, 5e4 [kg m2 s-1], used in the above shown plot was found empirically. Finding an optimal for all segments combined was deemed beyond the scope of this thesis. Observing a time trace created with the fixed amount of added damping, shows the improvement in a more insightful way, this is shown in figure 3.28.

Performance with Identified Coefficients Other Than Damping

Other coefficients were identified as well. None of the identified coefficients resulted in more accurate re-predictions, even when the updated coefficients were used to re-predict the section where they were identified from. As with the roll coefficients, using a coefficient that was identified in a preceding section lowered the performance, making that the identification procedure used was not able to improve the

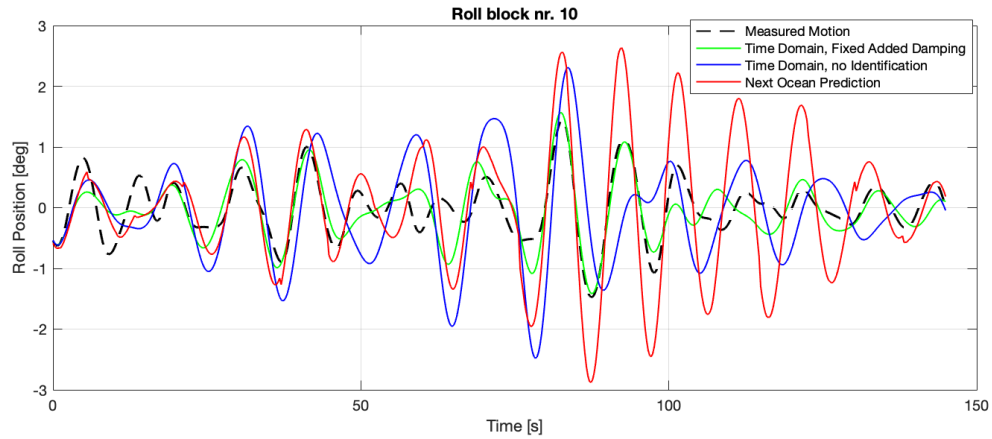

Figure 3.28: Adding the fixed amount of damping also visually improves the prediction quality.

predictions in any way.

The following force coefficients were identified:

- A sway acceleration induced roll moment.
- A roll acceleration induced roll moment.
- A roll position induced roll moment.
- A pitch velocity induced pitch moment.
- A roll velocity (to the first, second and third power) induced roll moment.

Correlation coefficients for re-predictions that have not been shown here are depicted in appendix D.

4

Discussion and Conclusion

Predicting wave induced vessel motions is of importance to safely execute complex operations at sea. Improving the accuracy of motion predictions increases the workability of vessels, thereby saving costs and increasing safety. Next Ocean makes motion predictions based on radar images of the surrounding wave field. These images are translated to motions using the Response Amplitude Operator; a function in the frequency domain. Consequence of this method is that no non-linear forces can be incorporated in the motion prediction. Aim of this project was to investigate if the use of added, nonlinear damping forces could improve the prediction of the roll motion. An attempt was done to identify the coefficients needed to determine these forces from vessel motion measurements. Roll is suspected to be relatively highly influenced by nonlinear damping forces. In order to incorporate these forces, an extended Cummins equation was used; a non linear equation of motion in the time domain.

4.1. Time Domain Modelling

Modelling wave induced ship motions in the time domain proved to be more cumbersome than motion modelling in the frequency domain. Complications may arise from the requirements on the hydrodynamic database; in order to use these commonly available and frequency dependent coefficients for time domain predictions, they should be accurately known to a relatively high frequency, and with a high frequency resolution. These requirements do not need to be fulfilled when the same coefficients are used to make predictions in the frequency domain. The average hydrodynamic database is therefore not suited to perform time domain predictions. For the Acta Auriga, the ship investigated in this project, the surge-heave damping curve was not resolved correctly, while more than average data for this vessel was available. Also, the hydrodynamic database would ideally have contained coefficients up to a higher maximum frequency, and with a smaller frequency step. This makes the use of time domain modelling cumbersome in Next Ocean's daily practises. Re-calculating the hydrodynamic coefficients to obtain a better hydrodynamic database is possible, but a panel model of the hull is needed for this. Also, for every ship the damping curves should be examined and although the tail fitting can be made to be an automated process, manually reviewing if the fit went as supposed is important to gain confidence in the to be created time domain predictions. These practical inefficiencies are a downside to using time domain modelling and limits the usefulness for Next Ocean, as their interest lies in easily scalable services.

Further limitations of time domain modelling are embodied by the poor modelling of degrees of freedom that do not have a restoring coefficient, i.e. surge, sway and yaw motions. Next Ocean is now mainly interested in the other degrees of freedom, however, clients with more stringent demands on surge, sway and yaw predictions may arise. Only the Acta Auriga was investigated in this project, other vessels may show a different running away behaviour. Predictions for vessels where the running away behaviour is more severe may suffer from the influence of cross terms to the heave, roll and pitch motions. It was found that the running away behaviour could be mitigated by adding damping to the concerned degrees of freedom. Adding extra damping made these DOF's time domain results match with frequency domain results accurately. The predicted motion amplitude was altered by the added

damping.

Furthermore, roll showed unstable motions when in free decay. This made that modelling the vessel that was excited by a spectrum could also be unstable when frequencies around the natural frequency were strongly represented in the spectrum. Only when adding more roll damping, these spectrum excitations could be kept stable. When damping was added, a close match between the frequency and time domain results was obtained for all excitation spectra. Adding damping did alter the modelled motion amplitude. In order to be able able to use spectrum excitation in the time domain model, an amount of damping must thus be found that eliminates the instability, but does not lower the response amplitude too much.

For roll, the damping obtained with the retardation function was positive. The phase between the retardation force and the motion velocity was more closely examined. The hypothesis that having this phase difference smaller then $\pi/2$ [rad] would make for unstable predictions, was rejected. Here too, adding damping made for a stable prediction and a more close match between the time and frequency domain, especially for spectrum excitations. For roll, no full understanding of the instability during free decay tests was gained. Plots (figure 3.7) showed that the total energy in the system grew, and that the work done by the inertia, retardation and restoring forces accounted for all energy in the system. How the retardation force added energy to the system was not understood.

The above described instabilities made straightforward use of time domain modelling difficult, even when the hydrodynamic database was not to pose any complications. Each vessel should be looked at individually and might need attention to make the simulations work appropriately.

From the above, it was concluded that performing time domain predictions in real time was not likely to be an improvement on real time frequency domain modelling, if at all feasible. In order to be able to use nonlinear forces in the equations of motion, the Cummins equation is to be used, as the frequency domain model is not able to incorporate nonlinear forces. Not being able to use the time domain in real time therefore means not being able to account for quadratic or cubic damping forces. However, coefficient identification may still be useful, as linear damping might improve predictions, especially for roll. Besides damping, other linear force coefficients may be found using identification. The updated coefficients could then be used in frequency domain modelling.

4.2. Identification and Re-Prediction

Correlations between force and moment residuals and position, velocity and acceleration of relevant degrees of freedom were used to identify forces and moments that were eligible for coefficient identification. Force and moment residuals are the differences between the hydrodynamic and hydrostatic forces determined from measured vessel motions on the one hand, and the predicted excitation forces on the other. Originally, roll damping was aimed at for identification. Because of this initial interest, coefficients for this force were looked for, despite the fact that no strong correlation between the first, second and third power of roll velocity and roll moment residuals was found. All three coefficients in the proposed damping force polynomial, see equation 2.22, showed highly varying values, also reaching negative values. The fact that negative force coefficients were obtained made that coefficient identification was deemed unsuited for roll damping, since these make the re-predictions unstable. Also when the time domain simulations would be less fragile, this result shows that the used identification method is not a straightforward path to improved roll predictions.

Instead of identifying the optimal damping, re-predictions were also done using a fixed amount of added damping. This resulted in slightly better roll predictions than those obtained by Next Ocean. Although this introduces the possibility to slightly improve the roll predictions, no identification nor time domain modelling is needed for this. Finding the optimal amount of fixed damping to add was considered out of the scope of this thesis. The value used in this project, 5e4 [kg m2 s-1] was obtained using trial and error.

Besides identifying roll damping, coefficients for roll-and yaw acceleration induced roll moments, a roll position induced roll moment and a pitch velocity induced pitch moment were identified. None of these updated coefficients led to improved predictions. This could well have to do with the non orthogonality of the predictor variables; acceleration, velocity and position. The hope was that since multiple frequencies were present in the motion, the position and the acceleration would be independent enough to allow for sensible identification. This was not the case as identifying inertia forces would change the correlation between the hydrostatic forces and the force or moment residuals.

4.3. Overall Conclusions and Recommendations

The research objective was to investigate if motion predictions could benefit from time domain modelling using non linear damping forces. It can be concluded that the used procedure did not lead to improved predictions. Modelling in the time domain was deemed too cumbersome to be a viable option for commercial use by Next Ocean. Adding damping based on identification did not improve predictions, adding a fixed amount of damping did improve the correlation between predictions and measurements with 9.57% on average.

Next Ocean might benefit from this finding, though in a different way than was aimed for in this project. Adding frequency independent damping is straightforward in the frequency domain. Designing a method to determine the desired amount of added damping was not done in this project. This could be a sensible direction to perform further investigations.

The results from this investigation did result in more insight in the complexities of time domain modelling. A similar effort as described in this report might be sensible, when a method different from direct integration is used for the retardation convolution. It is however worthwhile to overthink the need for the more complex time domain model as this study showed that no large role for nonlinear forces could be found in the field data. This conclusion might drastically change when data collected during a more severe sea state is considered, as nonlinearities typically arise at higher motion amplitudes. It might be the case that these nonlinearities only arise at seastates where Next Oceans clients cannot operate all together; making more accurate predictions in those conditions not of interest for Next Ocean. Looking into field data from a wider variety of conditions and from multiple vessels is therefore recommended to draw more firm conclusions on the potential of nonlinear damping forces. Even without finding nonlinear forces to be present in the considered cases, the roll predictions did perform worse then predictions for other degrees of freedom. Looking wider then nonlinear forces alone is therefore reasonable. As was discussed extensively, the roll RAO is highly peaked, making the results produced with the RAO more susceptible to errors in the predicted wavefield. This holds for both amplitude and phase of the predicted motions; the RAO would give a highly different motion prediction if a predicted wave component has a slightly wrong frequency or direction. Performing a study on the sensitivity to the wave prediction error might therefore be sensible.

More attention to the identification scheme could improve results drastically and is therefore a logical improvement to the work done in this project. If no nonlinear damping forces are considered, this still holds for updating the force coefficients in the frequency domain equation of motion. This can be especially useful for vessels where the RAO is not determined accurately. It is worth mentioning that when no nonlinear forces are considered, the time domain model is not needed to perform the identification, which would make the procedure less cumbersome.

A

RAO Phase

The first appendix shows the differences in phase between the time and frequency domain calculations, for monochromatic excitation. First for uncoupled motions:

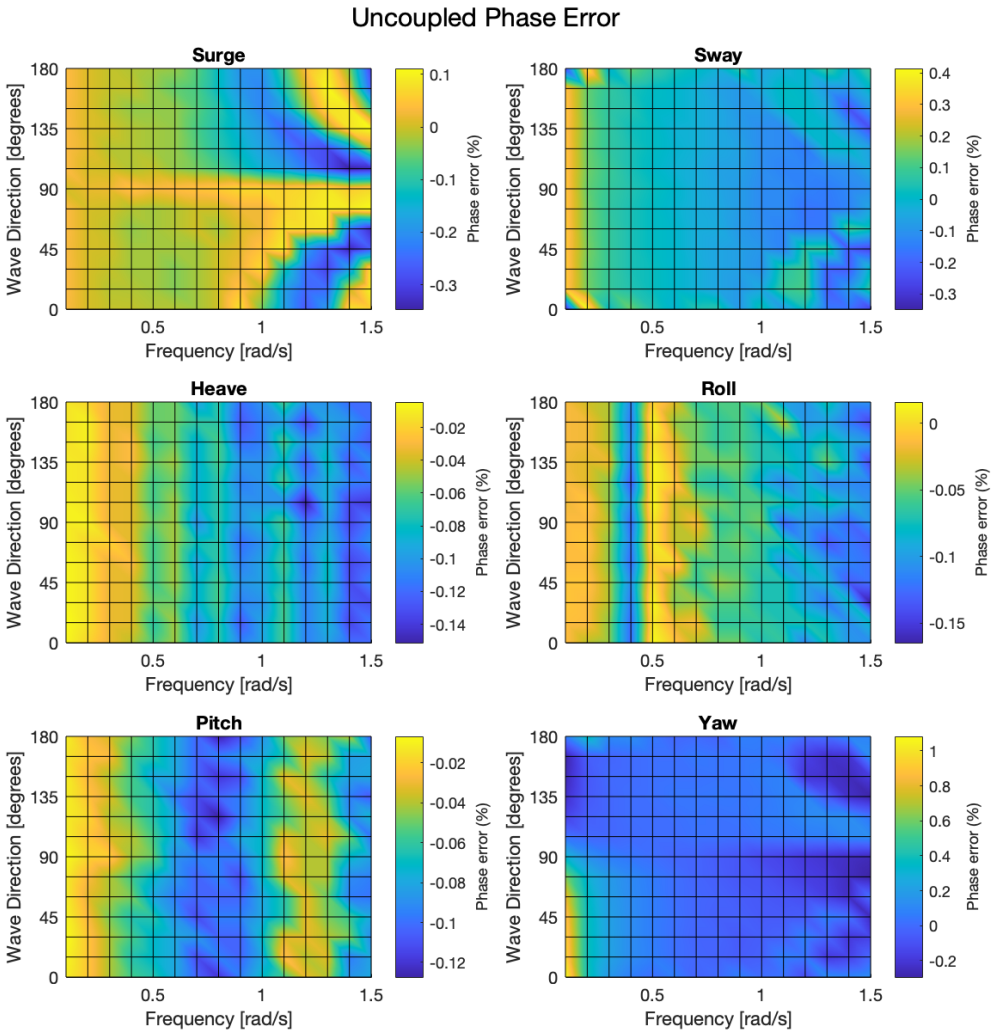

Also the coupled phase differences are shown:

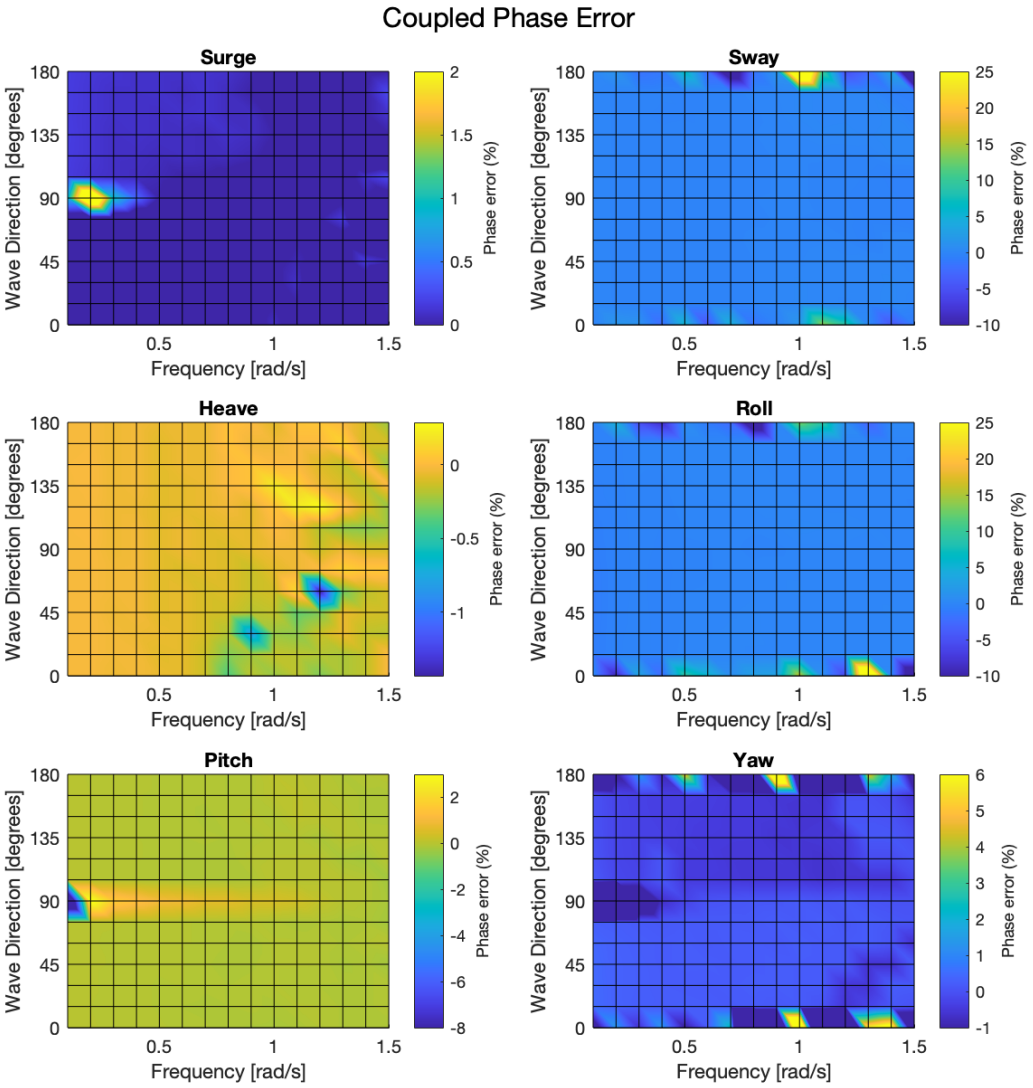

Figure A.1: Phase differences between time and frequency domain calculations. Values are in percentages. This is the percentage of the difference, relative to the frequency domain value. This also holds for the figure containing the differences of the uncoupled motions

B

Damping, Retardation and Added Mass

This second appendix shows plots of the damping curves, retardation functions and infinite frequency added masses, of both the diagonal and off-diagonal terms. First the damping curves:

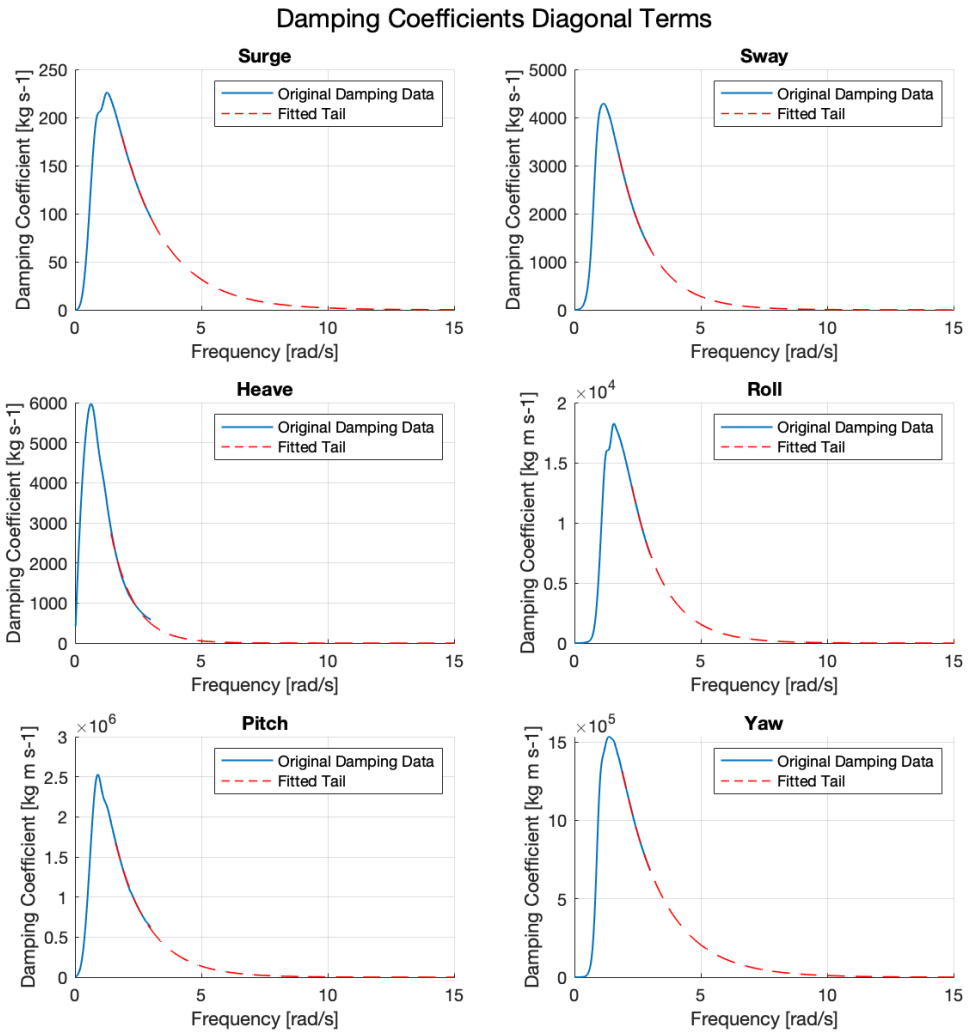

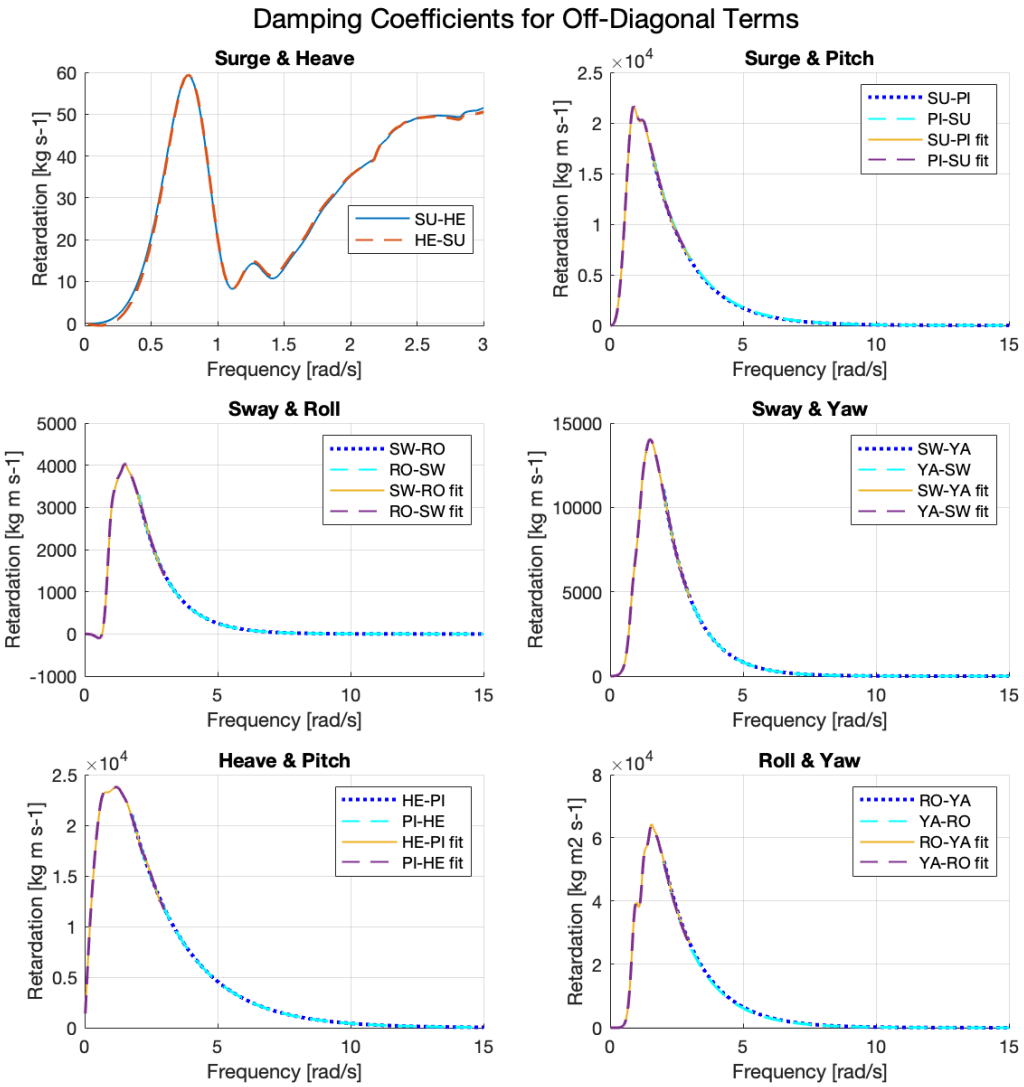
Damping Coefficients for Off-Diagonal Terms
Surge & Heave
Retardation [kg s-1]
Frequency [rad/s]
SU-HE
HE-SU
Surge & Pitch
×10^4
Retardation [kg m s-1]
Frequency [rad/s]
SU-PI
PI-SU
SU-PI fit
PI-SU fit
Sway & Roll
Retardation [kg m s-1]
Frequency [rad/s]
SW-RO
RO-SW
SW-RO fit
RO-SW fit
Sway & Yaw
Retardation [kg m s-1]
Frequency [rad/s]
SW-YA
YA-SW
SW-YA fit
YA-SW fit
Heave & Pitch
×10^4
Retardation [kg m s-1]
Frequency [rad/s]
HE-PI
PI-HE
HE-PI fit
PI-HE fit
Roll & Yaw
×10^4
Retardation [kg m2 s-1]
Frequency [rad/s]
RO-YA
YA-RO
RO-YA fit
YA-RO fit

From these damping curves, the retardation functions are calculated:

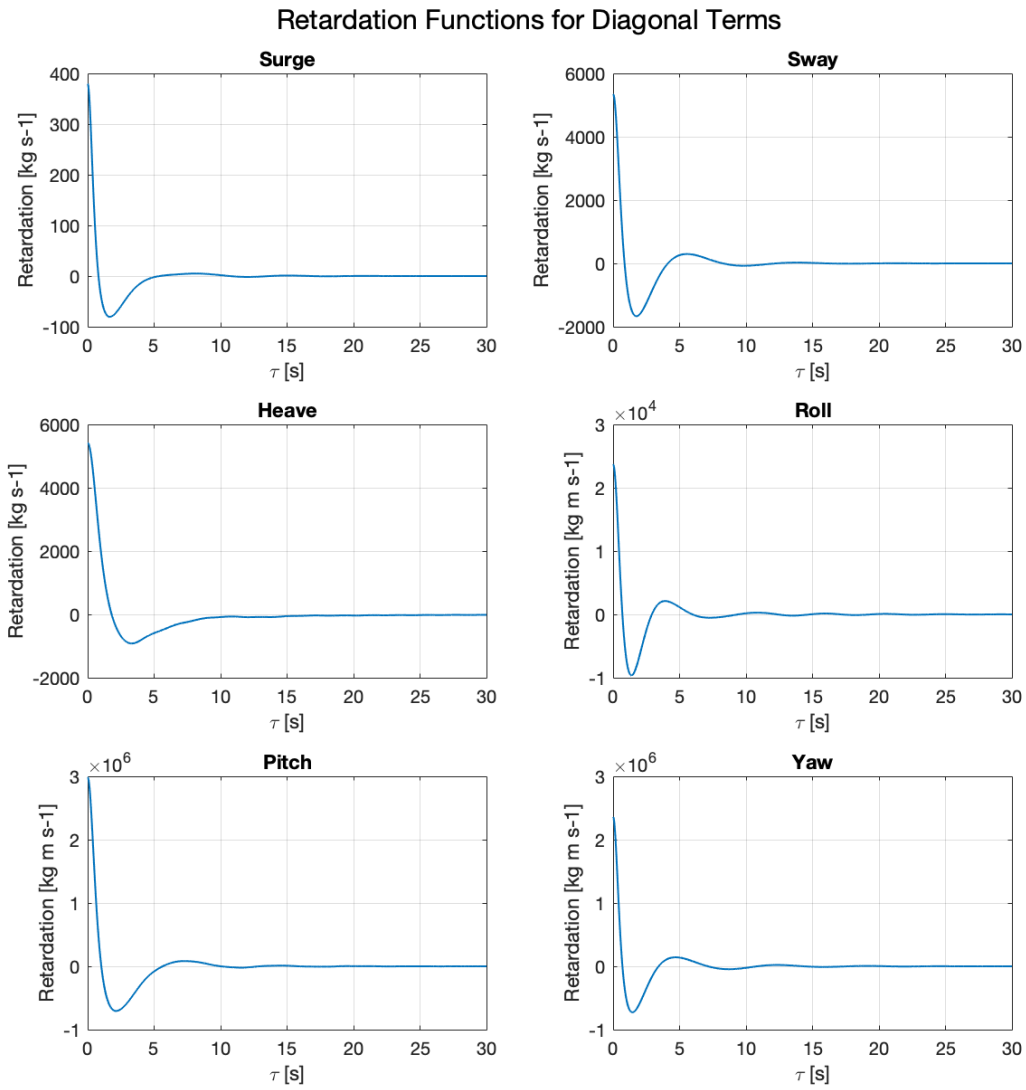

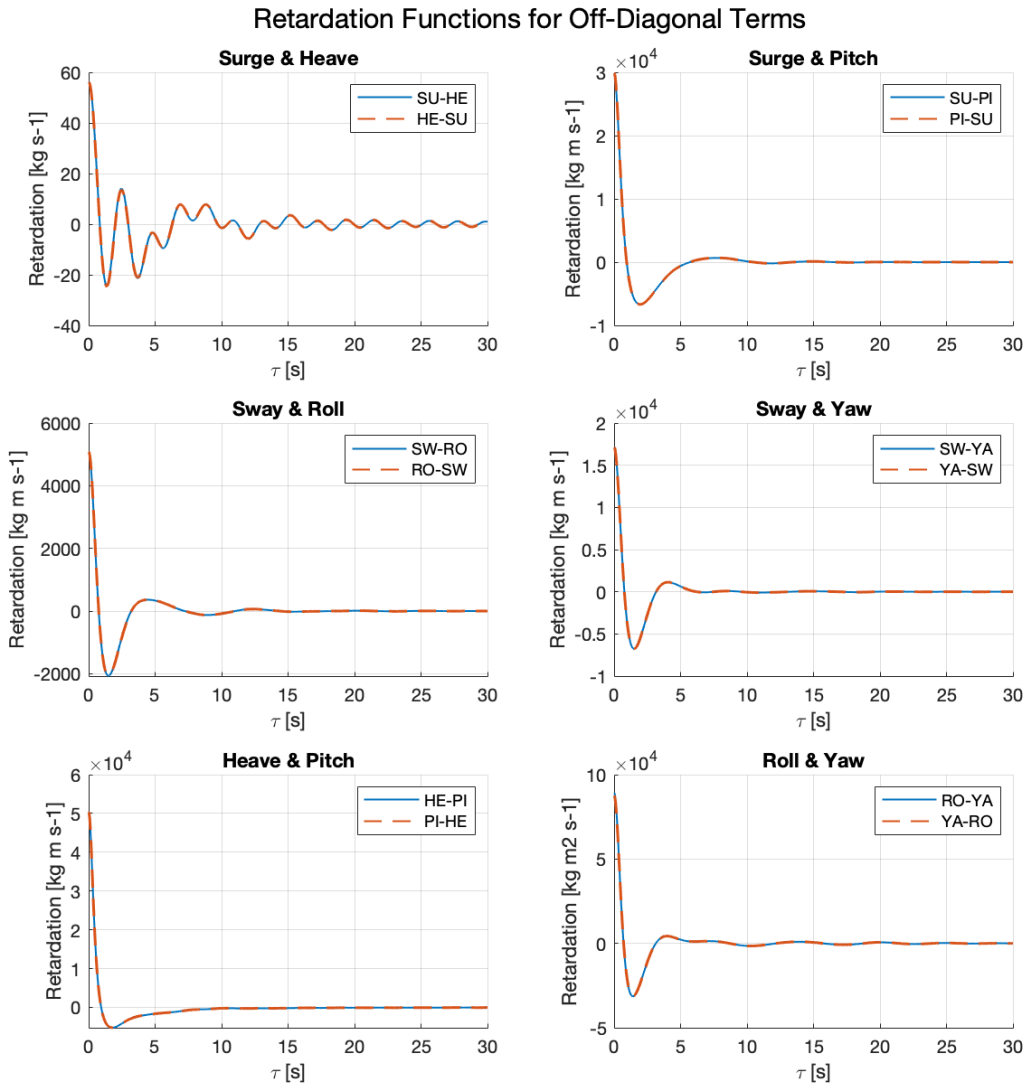
Retardation Functions for Off-Diagonal Terms
Surge & Heave
SU-HE
HE-SU
Retardation [kg s-1]
τ [s]
Surge & Pitch
SU-PI
PI-SU
Retardation [kg m s-1]
τ [s]
Sway & Roll
SW-RO
RO-SW
Retardation [kg m s-1]
τ [s]
Sway & Yaw
SW-YA
YA-SW
Retardation [kg m s-1]
τ [s]
Heave & Pitch
HE-PI
PI-HE
Retardation [kg m s-1]
τ [s]
Roll & Yaw
RO-YA
YA-RO
Retardation [kg m2 s-1]
τ [s]

From these retardation functions, the infinite frequency added masses were calculated:

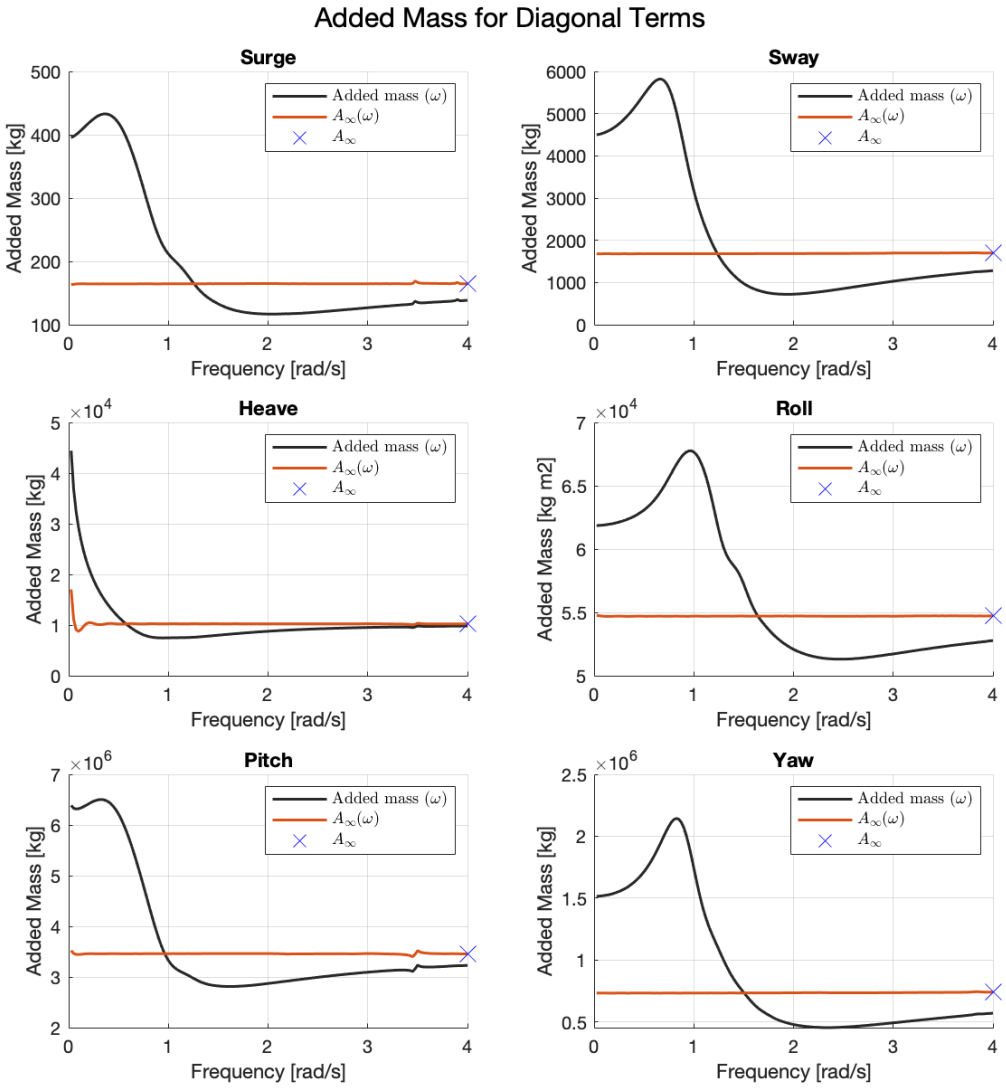

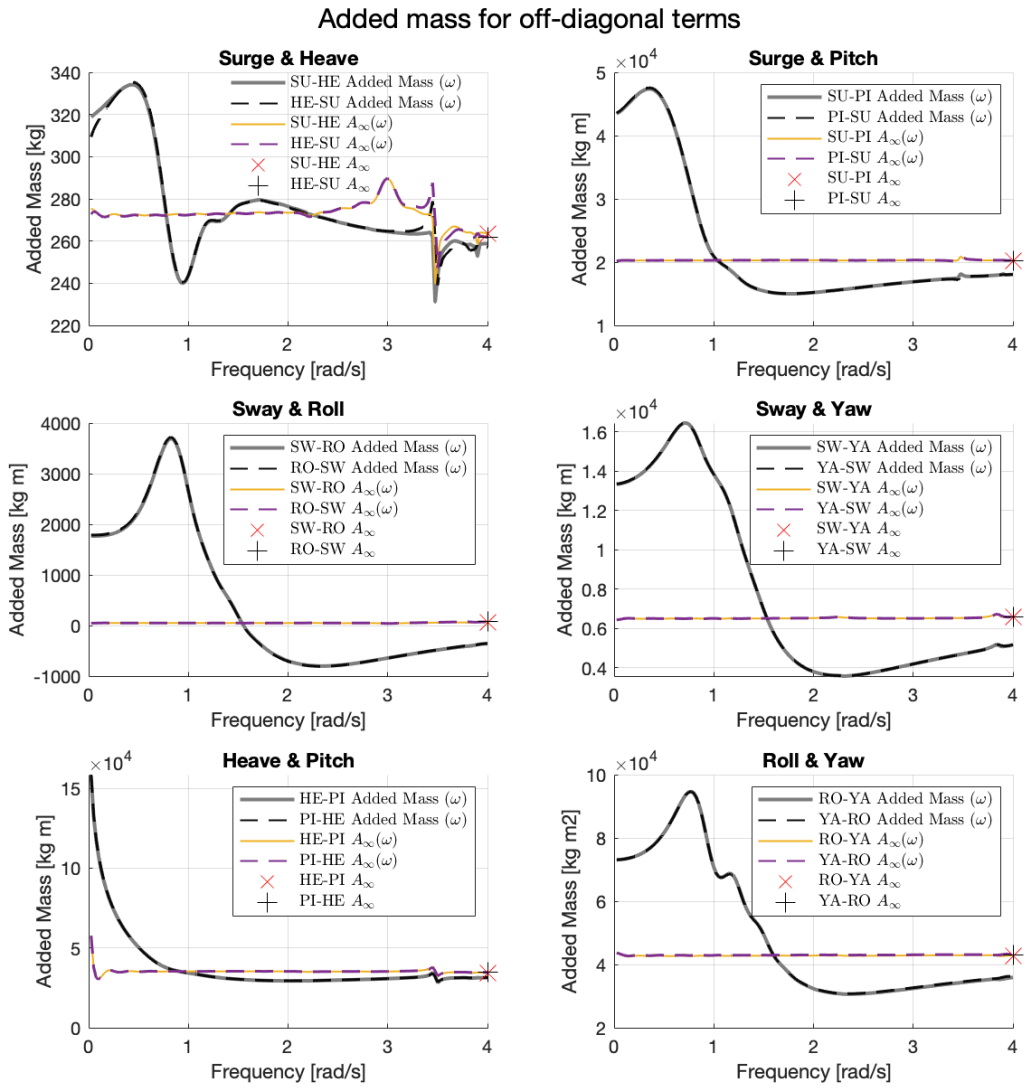
Added mass for off-diagonal terms
Surge & Heave
SU-HE Added Mass (ω)
HE-SU Added Mass (ω)
SU-HE $A_\infty(\omega)$
HE-SU $A_\infty(\omega)$
SU-HE A_∞
HE-SU A_∞
Added Mass [kg]
Frequency [rad/s]
Surge & Pitch
SU-PI Added Mass (ω)
PI-SU Added Mass (ω)
SU-PI $A_\infty(\omega)$
PI-SU $A_\infty(\omega)$
SU-PI A_∞
PI-SU A_∞
Added Mass [kg m]
Frequency [rad/s]
Sway & Roll
SW-RO Added Mass (ω)
RO-SW Added Mass (ω)
SW-RO $A_\infty(\omega)$
RO-SW $A_\infty(\omega)$
SW-RO A_∞
RO-SW A_∞
Added Mass [kg m]
Frequency [rad/s]
Sway & Yaw
SW-YA Added Mass (ω)
YA-SW Added Mass (ω)
SW-YA $A_\infty(\omega)$
YA-SW $A_\infty(\omega)$
SW-YA A_∞
YA-SW A_∞
Added Mass [kg m]
Frequency [rad/s]
Heave & Pitch
HE-PI Added Mass (ω)
PI-HE Added Mass (ω)
HE-PI $A_\infty(\omega)$
PI-HE $A_\infty(\omega)$
HE-PI A_∞
PI-HE A_∞
Added Mass [kg m]
Frequency [rad/s]
Roll & Yaw
RO-YA Added Mass (ω)
YA-RO Added Mass (ω)
RO-YA $A_\infty(\omega)$
YA-RO $A_\infty(\omega)$
RO-YA A_∞
YA-RO A_∞
Added Mass [kg m2]
Frequency [rad/s]

C

Force and Moment Residuals

This appendix shows the force and moment residuals for heave and pitch.

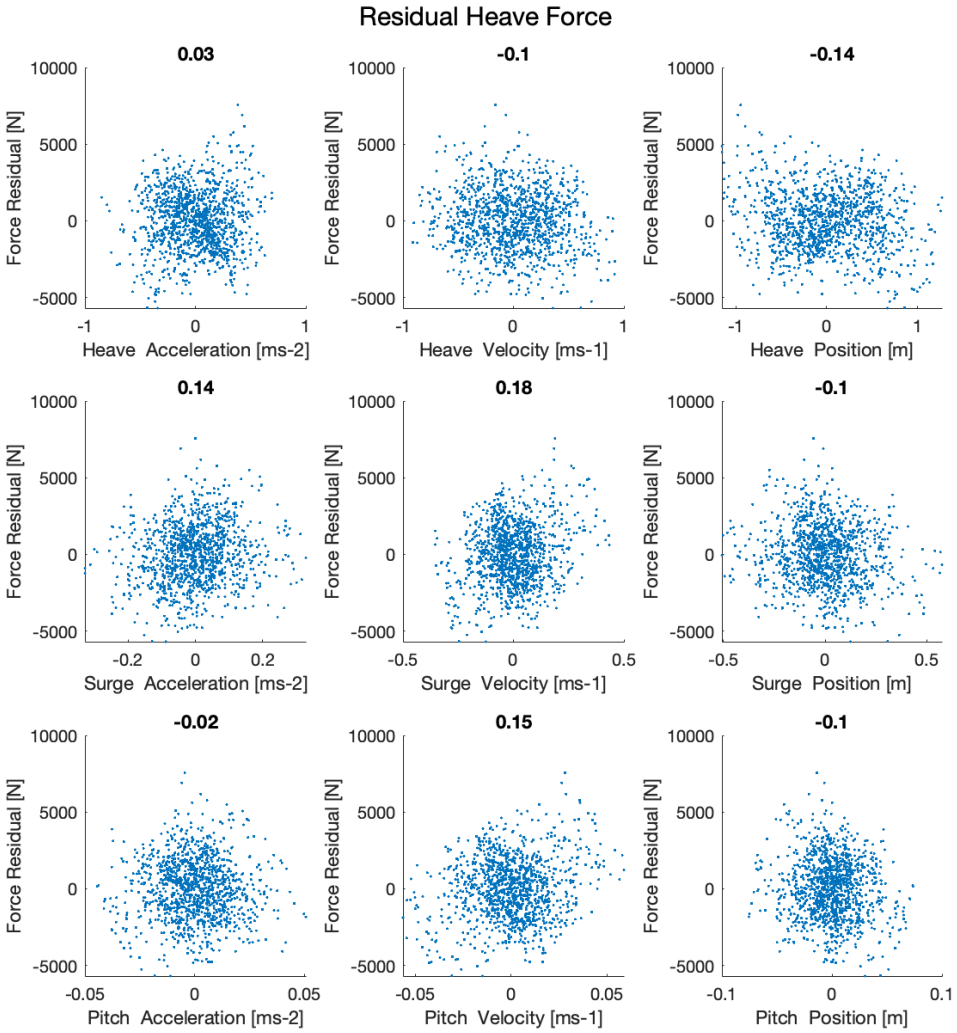

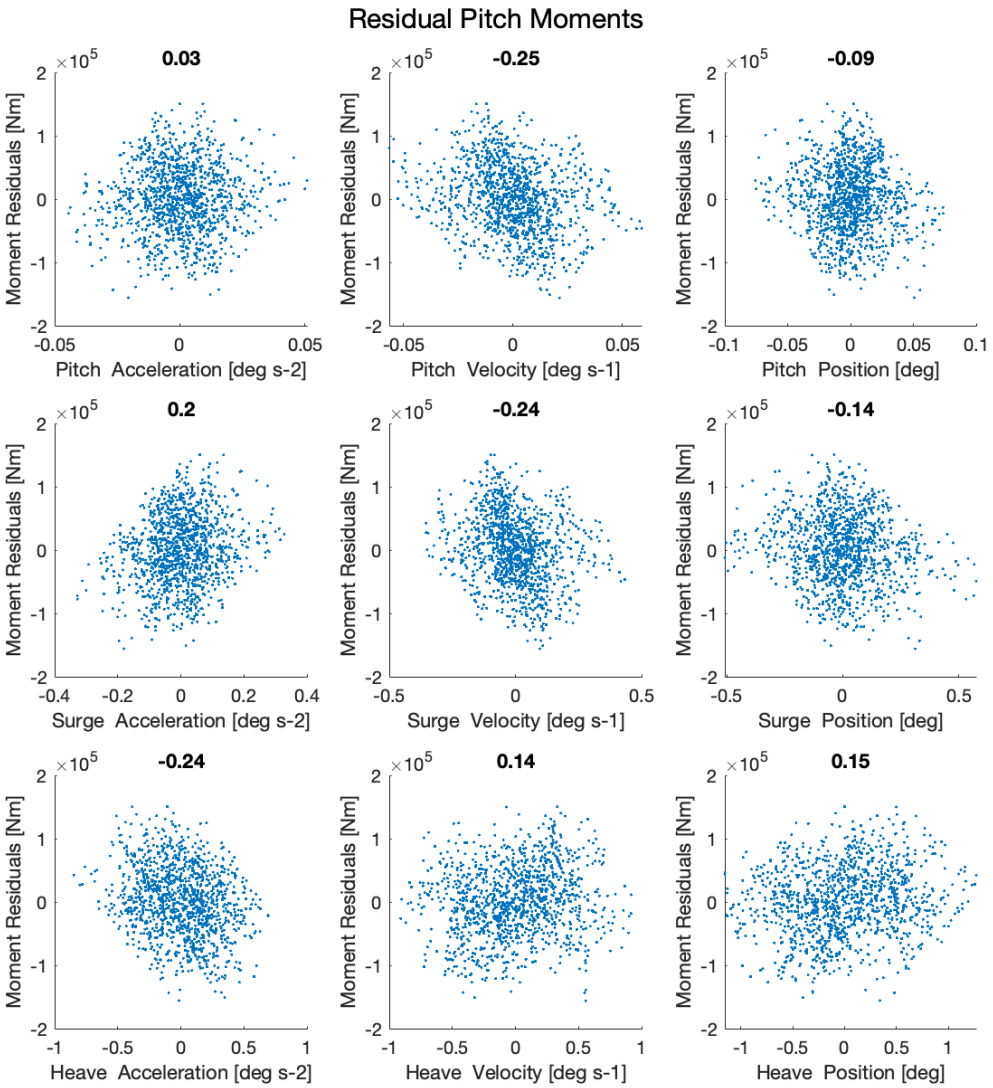
Residual Pitch Moments
0.03
-0.25
-0.09
0.2
-0.24
-0.14
-0.24
0.14
0.15
Moment Residuals [Nm]
×10^5
Pitch Acceleration [deg s-2]
Pitch Velocity [deg s-1]
Pitch Position [deg]
Surge Acceleration [deg s-2]
Surge Velocity [deg s-1]
Surge Position [deg]
Heave Acceleration [deg s-2]
Heave Velocity [deg s-1]
Heave Position [deg]

D

Correlation Coefficients of Re-Predictions with Identified Coefficients

The last appendix shows the correlation coefficients for re-predictions with new or updated coefficients.

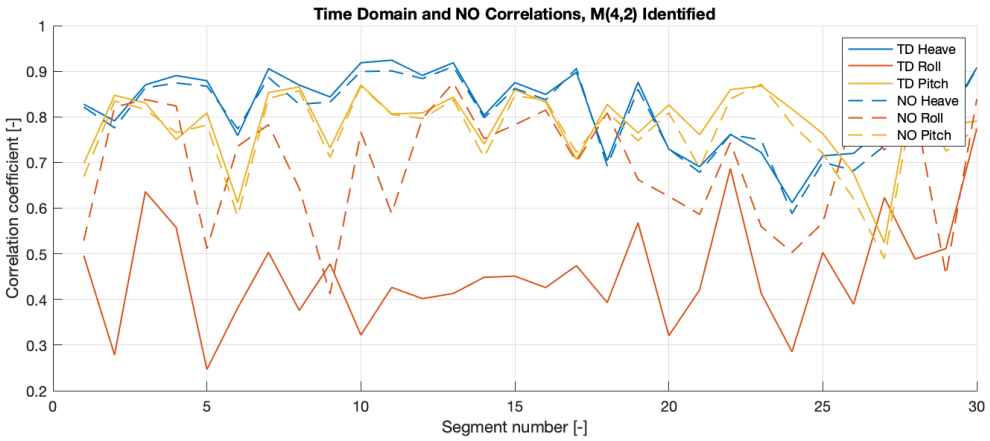

Figure D.1: Identification of a sway acceleration induced roll moment.

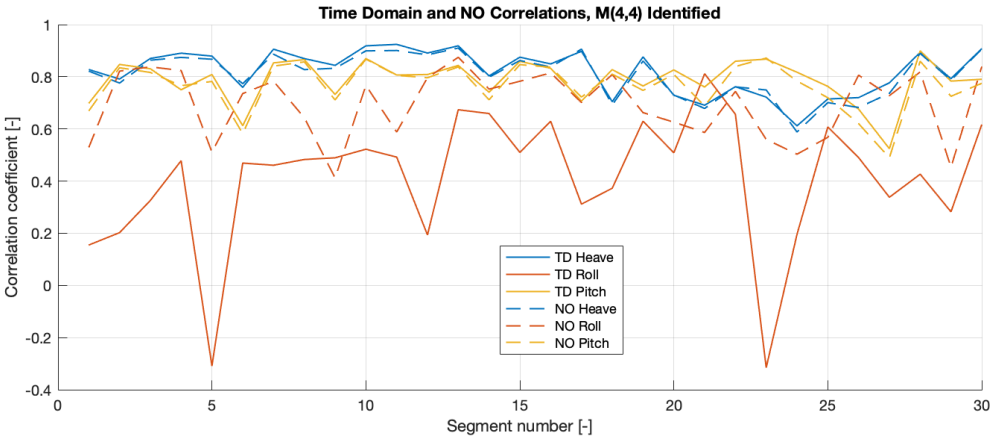

Figure D.2: Identification or a roll acceleration induced roll moment.

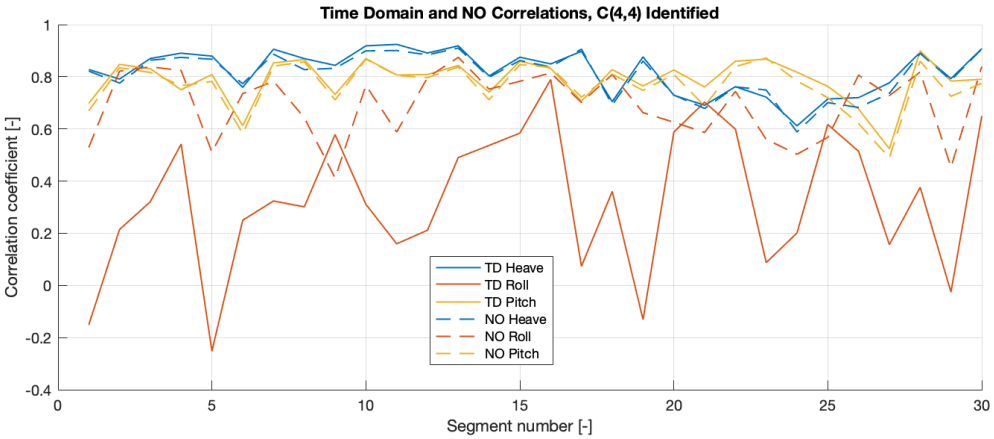

Figure D.3: Identification of a roll position induced roll moment.

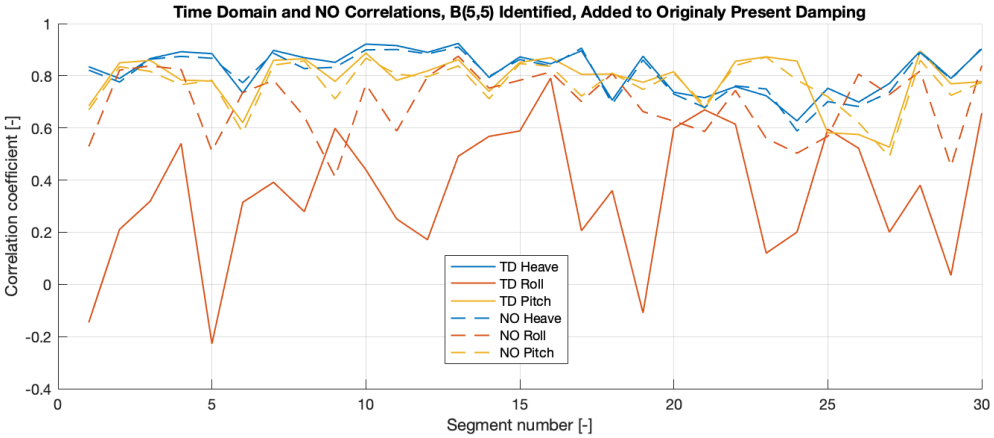

Figure D.4: Identification of a pitch velocity induced pitch moment.

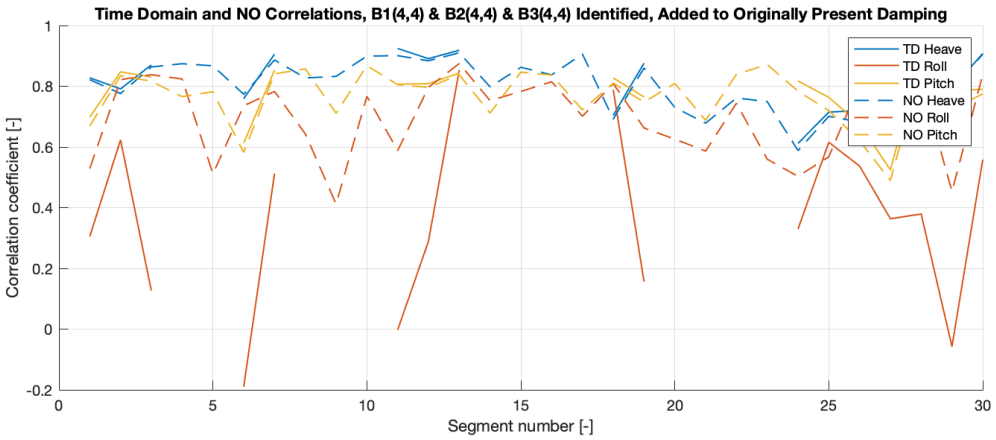

Figure D.5: Identification of added roll damping, linear, quadratic and cubic. Note the gaps in the re-predicted motion correlations. Negative damping has been identified and added in those segments, leading to unstable simulations.

Bibliography

[1] Hasmi A.N. “Time Domain Ship Motion without Convolution”. In: (2016).

[2] N. Borge. “Inversion of Marine Radar Images for Surface Wave Analysis”. In: (2004).

[3] W.E. Cummins. “The Impulse Response Function and Ship Motions”. In: (1962).

[4] Ma Y.; Sclavounos P.D.; Cross-Wither J.; Arora D. “Wave forecast and its application to the optimal control of offshore floating wind turbine for load mitigation”. In: *Renewable Energy* 128-A (2018), pp. 163–176.

[5] M.D.; Diez J.J.; Lopéz J.S.; Negro V. Esteban. “Why offshore wind energy?” In: *Renewable Energy, an International Journal* (2010).

[6] T. Fossen, ed. *Handbook of Marine Craft Hydrodynamics and Motion Control*. John Wiley Sons, Incorporated, 2011.

[7] R Gangeskar. “An Algorithm for Estimation of Wave Height From Shadowing in X-Band Radar Sea Surface Images”. In: *IEEE TRANSACTIONS ON GEOSCIENCE AND REMOTE SENSING* 52 (2014). DOI: 10.1109/TGRS.2013.2272701.

[8] Wijaya A.P.; Naaijen P.; Andonowati; van Groesen E. “Reconstruction and future prediction of the sea surface from radar observations”. In: *Ocean Engineering* 106 (2015), pp. 261–270.

[9] Leo H. Holthuijsen, ed. *Waves in Oceanic and Coastal Waters*. Cambridge University Press, 2010. ISBN: 9780521129954.

[10] Montazeria N; Nielsen U.D.; Jensen J.J. “Estimation of wind sea and swell using shipboard measurements – A refined parametric modelling approach”. In: *Applied Ocean Research* 54 (2016), pp. 73–86.

[11] Armesto J.A.; Guanche R.; del Jesus F.;Iturrioz A.; Losada I.J. “Comparative analysis of the methods to compute the radiation term in Cummins’ equation”. In: *Journal of Ocean Engineering* 1 (2015), pp. 377–393. DOI: 10.1007/s40722-015-0027-1.

[12] J.H.J. Journee. “Hydromechanic Coefficients for Calculating Time Domain Motions of Cutter Suction Dredges by Cummins Equations”. In: (1993).

[13] J.; W.W. Massie Journée, ed. *OFFSHORE HYDROMECHANICS*. Delft University of Technology, 2001.

[14] Li G.; Weis G.; Mueller M.; Townley S.; Belmont M. “Wave energy converter control by wave prediction and dynamic programming”. In: *Renewable Energy* 48 (2012), pp. 392–403.

[15] P Naaijen. “Navigational radar as decision support”. In: *SWZ MARITIME* 132 (2011).

[16] U.D. Nielsen. “Estimations of on-site directional wave spectra from measured ship responses”. In: (2006).

[17] T.F. Ogilvie. “RECENT PROGRESS TOWARD THE UNDERSTANDING AND PREDICTION OF SHIP MOTIONS”. In: (1964).

[18] R. Pascoal. “Estimation of directional sea spectra from ship motions in sea trials”. In: *Ocean Engineering* 132 (2017), pp. 126–137.

[19] Al-Habashneh A.A.; Moloney C.; Gill E.W.; Huang W. “An Adaptive Method of Wave Spectrum Estimation Using X-Band Nautical Radar”. In: *Remote Sensing* 7 (2015). DOI: 10.3390/rs71215851.